TRANSPORT-REGIME IN THE WESTERN TROPICAL INDIAN OCEAN

J R DONGUY[1]
and
GARY MEYERS
CSIRO Division of Oceanography
GPO Box 1538
Hobart TAS 7001 Australia

1. Visiting scientist, permanent affiliation: ORSTOM, France

Abstract

In the western Indian ocean, dynamic height has been calculated from XBTs collected along several shipping routes. In the northern hemisphere, low dynamic heights prevail during the NE monsoon and high dynamic heights during the SW monsoon inducing an alternating Somali Current. In the southern hemisphere, at 7° - 8°S a trough of low dynamic height occurs during the whole year. EOF analysis is used to document the variation of these features.

The geostrophic transports calculated on the XBT routes show spatially coherent patterns with strong seasonal variations. In the Arabian Sea, a counterclockwise gyre develops during the NE monsoon alternating with a clockwise gyre during the SW monsoon. Between 5°N and 5°S, the transport variations show eastward flow twice each year during the monsoon transitions, except on the westernmost route where the annual variations of the gyre in the Arabian Sea extends to the equator. The mean transport of the South Equatorial Current increases regularly with longitude from east to west in all months. It has small annual variations and the phase of the annual maximum progresses consistently westward.

1. Introduction

It is recognised that the southern hemisphere oceans are less sampled and less studied than the northern hemisphere oceans. This is particularly true for the southern Indian Ocean. Observations collected recently under auspices of the international Tropical Oceans and Global Atmosphere (TOGA) Programme and the World Ocean Circulation Experiment (WOCE) have added substantially to the large scale coverage of thermal (baroclinic) structure.

Historical observations tended to be sparse, or highly localized. The International Indian Ocean Expedition was carried out during 1962-1965 (WYRTKI, 1971) and showed that the north western Indian Ocean, is dominated by the monsoon. The strong response in ocean currents attracted a number of studies through the 1970's and early 1980's that focused on the currents and eddies off the coast of Somalia. The results have been comprehensively reviewed by KNOX (1987). A highlight was the description by DUING et al. (1980) and SWALLOW and FIEUX (1982) who pointed out the behaviour of the surface flow of the

Somali Current, which sometimes forms two gyres off the eastern coast of Africa. The study of western boundary currents was extended to higher latitudes by DONGUY and PITON (1991), showing that circulation in the Mozambique Channel is also characterised by a seasonal cycle of meridional transport in phase with the monsoon cycle. The East African Current and other boundary currents located in the vicinity of Madagascar have been described by SWALLOW et al. (1988), SCHOTT et al. (1988) and SWALLOW et al. (1991) who document the transport, the seasonal regime and the possible monsoon influence.

The large scale description of currents including the early works of WYRTKI (1973a, 1973b) and the recent study by MOLINARI et al. (1990) used surface-drift measurements to generate a monthly climatology of surface currents. They documented reversing monsoon currents, particularly in the northern hemisphere, and strongly semiannual variations in the current on the equator. These studies were representative primarily of the directly wind driven currents. Variation in subsurface thermal structure associated with the monsoons was described by COLBORN (1975). HASTENRATH and GREISCHAR (1991) used historical oceanographic observations from atlases to define the pattern of currents and the influence of the monsoon on large scale surface currents, including a partition into geostrophic and wind driven components. WOODBERRY et al. (1989) using a reduced gravity-model found that the main feature in the southern hemisphere is a cyclonic gyre including the South Equatorial Current and South Equatorial Countercurrent.

This study is concerned with a large scale description of upper layer transports in the Arabian Sea and western tropical Indian Ocean using new expendable bathythermograph (XBT) data. It extends the earlier climatological studies by focussing on the subsurface, geostrophic circulation which develops in response to monsoon winds. The observations were made routinely and systematically during a period of three years, 1986 - 1989.

2. Data and data processing

Since 1983, the TOGA/WOCE XBT Programme in the Indian Ocean has been gradually extended by Australia (CSIRO), France (ORSTOM) and Japan (JMA) over the following routes:

Port Hedland (20°S, 118°E)-Japan	(since 1985)
Fremantle-Sunda Strait	(since 1983)

Fremantle-Persian Gulf	(since 1986)
Fremantle-Red Sea	(since 1986)
Red Sea-Reunion Island (21°S, 55°E)	(since 1985)

The first two routes cover the eastern Indian Ocean and have been used for studies of the Pacific-Indian Ocean throughflow (MEYERS, 1992; MEYERS et al., 1993a). The three last routes cover the western Indian Ocean, (20°S-25°N, 50°E-90°E) and are used for the present study. Sampling on the northern end of the route to the Persian Gulf was stopped near 17°N in the early years of the programme due to the Iran-Iraq War. The TOGA/WOCE XBT Programme added several additional lines to the Indian Ocean after 1989 which are not included in this study. Sampling on a line along the eastern coast of Africa was unfortunately stopped before the TOGA programme began, and was subsequently started again. Clearly, a climatology based on much more data can be prepared at the end of TOGA; however, the data collected during the first years is enough to produce a representative climatology which will be useful for descriptive purposes and for the validation of general circulation models which are being developed.

XBTs provided temperature profiles from the surface to 450m (or more) every 60 - 90 miles along the routes. Bimonthly, averaged values of temperature at standard depths, dynamic height and the geostrophic transport function relative to 400 db have been computed to study qualitatively and quantitatively the distribution of currents during a standard year. The data used for the climatology covered the period 1983 thru 1989. Preparation of the climatology is described in detail in a report (MEYERS et al., 1993b). Briefly, the averages along a route were calculated in bins of one degree of latitude, except near coastal boundaries where bins were adjusted to have one in shallow water (<500 m) when possible. With the exception of one line, no spatial smoothing was permitted so that the consistency of the seasonal cycle in adjacent bins could be checked. The Fremantle-Persian Gulf line was processed with overlapping 3° latitude bins because it was not covered as consistently as the others. The averages were calculated for bimonths with a one month overlap (January-February, February-March, etc.) Dynamic height and the transport function were calculated from the bimonthly averaged temperature using the climatological temperature/salinity relationship (LEVITUS, 1982). The dynamic height-profiles along the routes were presented in a preliminary study by DONGUY and MEYERS (1992).

3. Seasonal variation of dynamic height

According to the general description of the surface circulation in the western tropical Indian Ocean by WYRTKI (1973a) and MOLINARI et al. (1990), the region is characterized by reversals of the major currents in response to monsoons. The currents with the strongest monsoonal variation are the Somalia Current (SC), which flows strongly northward along the coast of Africa during the SW monsoon (June to September) and southward during the NE monsoon (December to February); and the North Equatorial Current (NEC) south of India, which flows westward during the NE monsoon and eastward during the SW monsoon, when it is sometimes called the Indian Monsoon Current (IMC). Annual variation without reversal was also noted in the South Equatorial Countercurrent (SECC) and the South Equatorial Current (SEC). The SEC and SECC form a distinct gyre in the southern hemisphere (MOLINARI et al., 1990). Bimonthly charts of the surface dynamic height relative to 400 db determined from the XBT data (Fig.'s 1 and 2) indicate a circulation pattern which is generally consistent with this scheme; however closure of the gyres at the western boundary cannot be seen because of the lack of data near the coast of Africa.

The charts show that dynamic height in the Arabian Sea from December to February is characterised by a low indicating counterclockwise circulation and by the southwestward SC along the African coast (Fig. 1). The low is associated with the presence of cool, saline water originating from the Arabian Sea in the northern winter during the NE monsoon (DONGUY 1974). The full sequence of charts (not presented) shows that the low is a transient phenomenon and is quickly replaced by a high in March. A broad low in the southern hemisphere near 8°S is the trough between the SEC and the SECC. The trough extends into the central Indian Ocean, which might be expected due to the usual location of the Intertropical Convergence Zone (ITCZ) south of the equator in this season, but it is a weak feature. Bimonthly dynamic height charts from the International Indian Ocean Expedition (WYRTKI, 1971) present a similar pattern for the season of the NE monsoon.

The dynamic height from June to October during the SW monsoon is characterised by a strong high in the Arabian Sea and again the low SECC trough in the southern hemisphere (Fig 2). The high indicates clockwise circulation around a gyre in the Arabian Sea and the northeastward Somali Current. The maximum dynamic height is located near 10°N and includes the Great Whirl described

by SWALLOW and FIEUX (1982). The high is associated with warm, low salinity water coming from the equatorial area of the western Indian Ocean (DONGUY, 1974). The high is a more persistent feature than the previous low, lasting five months instead of three. The trough between the SECC and SEC clearly extends into the central Indian Ocean in this season. The SECC flows against the prevailing wind and in this sense appears to be dynamically similar to the Countercurrent in the Pacific Ocean (MEYERS, 1979). Bimonthly dynamic height charts from WYRTKI (1971) present a similar pattern for the SW monsoon also.

The complete set of dynamic height maps showed that the SECC trough has maximum eastward extension during the transition season April-May (Fig. 3), reaching at least 90°E. This feature may be related to the presence of the ITCZ at 10°S for five months, and it comes at the end of the season of westerly winds between the equator and 10°S. The SECC flows in the direction of the wind during the five months. Again, the appearance of the trough in this season is in good agreement with WYRTKI (1971). The high dynamic height of the Arabian Sea has already developed by April-May and suggests a clockwise circulation including the NEC and the SC.

The variation of dynamic height throughout the year was represented by empirical orthogonal functions (EOF) using the data for all the XBT lines listed above. The EOF results west of 90°E are presented to document the annual variation in the Arabian Sea and tropical Indian Ocean. The EOF results (Fig.'s 4 and 5) show temporal variation with peak monsoon development near January - February and July - August, and a secondary peak in the first EOF in April - May. The dynamic height fields at these times were presented Figures 1-3.

The first EOF (Fig 4) represents primarily variations of the monsoon gyre north of the equator and a change in the meridional slope of dynamic height across the SECC and SEC. It accounts for 43% of the monthly variance. The associated time function describes one asymmetric cycle per year, which shows the longer persistence of the pattern of circulation for the SW monsoon, and the rapid formation and decay of the pattern for the NE monsoon. From March thru October, a high deviation fom the mean dynamic height develops at 5°N, 55°E, representing the centre of variation of the gyre. The circulation around this core is clockwise in this season. South of the equator, the eastward current is strengthened

in both the western and central Indian Ocean. This pattern appears to begin in March/April before the onset of the SW monsoon suggesting that its dynamics is not controlled by the local wind. The EOF suggests that the counterclockwise circulation during the NE monsoon develops for a relatively short period from November thru February.

The second EOF shows dynamic height variations concentrated near the western boundary particularly in the northern hemisphere. It represents 34% of the variance (Fig 5). It seems to represent the patterns during the peak and mature phases of the monsoons. The pattern is largely devoted to the Somali Current and the SECC trough on the routes closest to the western boundary. The third EOF (not presented) represents 10% of the variance and seems also devoted to the Somali Current. The associated time function describes two cycles per year.

4. Seasonal variations of the 0-400 db transport

The large scale Indian Ocean circulation was described by WYRTKI (1973a) and MOLINARI et al. (1990) using primarily surface drift currents. The XBT data can be used to document the associated, relative geostrophic flow in the layer 0 to 400 m. Using the profiles of net geostrophic transport function along the tracks, the boundaries of currents were identified (Fig.'s. 6 and 7, dots) by choosing regions where the prevailing current had a consistent direction. The volume transport relative to 400 db was then calculated for each current. The transports between 0.5°N and 0.5°S were ignored. Use of the differential form of the geostrophic relationship was rejected for this study because the three-year averages are still too noisy to calculate second derivatives of dynamic height. The transport between 0.5°S-2.5°S was considered as the southern component of the equatorial jets and the transport between 0.5°N-2.5°N as its northern component. The transport of the gyre in the Arabian Sea was assessed between 2.5°N and 7.5°N on the southern side and north of 7.5°N on the northern side off Somalia, while the boundaries of the gyre were shifted to the north slightly on the Fremantle-Persian Gulf line. The NEC/IMC was assessed on the Persian Gulf line between 2.5°N and 7.5°N (the latitude of Sri Lanka). The SEC was assessed between the subtropical ridge in dynamic height and the SECC trough. The SECC was assessed between 2.5°S and the SECC trough. Maps of the transports during the peak monsoon seasons are given in Fig's 6

and 7 in 10^6 m^3/s (Sverdrups, Sv) and arrows indicate the direction of flow inferred from the maps of dynamic height.

The transports for January/February (Fig. 6) show all of the major currents for the NE monsoon season discussed by Molinari et al. (1990). A new feature is a counterclockwise circulation in the Arabian Sea. The gyre is a coherent feature on all the transport maps for December to February (not presented), suggesting a relative gyre-transport during the peak monsoon of approximately 10 Sv. In February/March (not presented) the transport around the gyre weakens to 7 Sv. This gyre can also be seen in the transport maps of the Indian Ocean Atlas (WYRTKI, 1971. p. 382). The NEC flows westward south of the gyre and seems to turn north eastward (Fig. 1) to join the gyre in the western, equatorial region. The relative transport of the SEC is greater than 20 Sv and flows zonally across the three tracks apparently to the western boundary currents. A large part of it may join the SECC, which has a relative transport of 16 Sv on the westernmost track. Curiously, the SECC is a weak current on the two tracks in the central Indian Ocean throughout the period January to March, suggesting that much of the flow in the SEC/SECC gyre (MOLINARI et al., 1990) recirculates near the western boundary. It is necessary to note that the transport calculation is questionable in the vicinity of the equator and consequently the erratic estimates near the equator in Fig. 6 may be in part due to the aliasing of eddy variability.

The transport map for August/September also shows all of the major currents for the season (Fig. 7). From July to October, the circulation pattern shows a clockwise gyre in the Arabian Sea, intensified in the west, in the feature historically called the Great Whirl (GW). The gyre appears as a coherent feature on all the transport maps from July thru October (not presented) with a typical relative transport of 20 Sv circulating around the GW. The gyre shifts measurably northward during the SW monsoon and by September is located entirely north of 5°N. Again, the gyre-transports during the peak monsoon (Fig. 7) are in agreement with the the Indian Ocean Atlas (WYRTKI, 1971. p. 385); and the circulation pattern is consistent with later studies of the Somalia Current (SWALLOW and FIEUX, 1982). Outflow from the eastern end of the gyre seems to feed the IMC (Fig.'s 2 and 7). In the southern hemisphere the SECC is strong (19 Sv) in the West and considerably weaker in the central Ocean, suggesting recirculation. Transport of the SEC is about 20 Sv, as it was during the opposite

monsoon. And again, some noisy transport vectors appear near the equator.

Time series (Fig.'s 8-12) were prepared to describe variations of the major currents. The annual variations of the Somali Current north of 7.5°N are clearly documented (Fig. 8) on the Red Sea lines. Sampling on the route to the Persian Gulf was unfortunately not permitted close to the coast during the period of this study and the extension of the Somali Current into the northern Arabian Sea could not be monitored. The three lines give a clear representation of variations in the SC and the gyre in the Arabian Sea. The annual cycle of relative transport in the Somali Current on the two Red Sea lines (Fig. 8, left and middle panels) varies from northeastward during May to November with a peak >20 Sv, to southwestward from November to May with a trough of 15 Sv. The return flow from the Somali Current circulates around the gyre and crosses the sampled part of the Persian Gulf line flowing in the opposite direction off the southern coast of India (Fig. 8, right panel). The magnitude of variations in the eastern gyre is considerably smaller than in the SC. The transport variations on the southern side of the gyre on the Reunion-Red Sea line (Fig. 9, left panel) are consistent with the observations of the Somali Current (i.e. the direction is reversed and magnitude about the same). The reversal is also apparent on the Fremantle-Red Sea line (Fig. 9, right panel), but higher frequency variations also appear.

Strong annual variation of the NEC/IMC was observed on the Fremantle-Persian Gulf line. The transports (not presented) were essentially bimodal with westward flow averaging >10 Sv during February thru May and eastward flow averaging >5 Sv during July thru November. The strong monsoon variation in this region has been noted in numerous earlier studies, and on the basis of surface drift data it was usually linked directly into the Somali Current system (WYRTKI, 1973a; MOLINARI et al.,1990) and its associated gyre. The geostrophic transports (Fig.'s 6 and 7) suggest that the gyre is a nearly closed circulation with the NEC flowing into it during the NE monsoon and the IMC flowing out of it during the SW monsoon.

The semiannual eastward jets on the equator (WYRTKI, 1973a; MOLINARI et al., 1990) appear coherently in transport estimates between 2.5°S and the equator (Fig 10). The time series along the three shipping routes show peaks of eastward transport during the transition seasons with a stronger peak exceeding 15 Sv

in the May transition and a weaker peak exceeding 5 Sv in the October transition. Between 2.5°N and the equator (Fig. 11), the transport on the easternmost line (Fremantle-Persian Gulf) is semiannual and in phase with the jets on the southern side of the equator (Fig. 10). Conversely, the transport between 2.5°N and the equator on the Reunion-Red Sea line has an annual cycle because it is influenced by the monsoon gyre of the Arabian Sea. Thus it is in phase with the return flow of the Somali Current shown in Figure 9. A strong eastward flow is discernible on the Reunion-Red Sea line in October but it does not appear on the Fremantle-Red Sea line. Variations on the Fremantle-Red Sea line between 2.5°N and the equator have a strong semiannual component in phase with the equatorial jets but the annual component is difficult to interpret.

The SECC is a prominent feature of the southern Indian Ocean circulation and is expected to have an annual cycle associated with the ITCZ. Its transport was calculated between 2.5°S and the Countercurrent trough located between 5° and 10°S, without trying to distinguish it from the equatorial jets. The eastward transport (Fig. 12, top) in the central ocean (Fremantle-Persian Gulf and Fremantle-Red Sea lines) is maximum in April/May when the trough is well developed (Fig. 3). The maximum occurs at the end of the season of westerly winds between the equator and 10°S, when the ITCZ is displaced southward. The maximum matches the phase of the May peak of the semiannual equatorial jet (Fig. 10) which probably merges with the SECC at this time. The transport in the western ocean (Reunion-Red Sea line) has a weak maximum somewhat later during June thru August and a smaller annual amplitude. The variations in transport on all three lines closely match the phase of changes in dynamic height at the Countercurrent trough. The latitude of the trough (Fig. 12, bottom) is between 5°S and 10°S in the westernmost line, between 3°S and 7°S in the central one and varies between 4°S and 11°S in the easternmost line with an abrupt change from 11°S to 4°S between July and August.

The South Equatorial Current is the most powerful and persistent current in the tropical Indian Ocean (HASTENRATH and GREISCHAR, 1991) and is easily identified on temperature sections from the topography of the thermocline. Its latitude changes slightly with longitude but stays between 20°S and 5°S. The transport functions estimated from XBT were used to document the strength of the SEC all across the Indian Ocean (Table 1). On the Port Hedland - Japan line, the westward flow is between 13°S and

9°S and its mean relative transport is 5.5 Sv at 123°E. On the Fremantle - Sunda Strait line it is between 15°S and 7°S, and has a mean transport of 9.2 Sv at 106°E. (Note that the average covers the eastward South Java Current as well as the SEC in this latitude band. See Meyers et al., 1993a for more details.) On the Fremantle - Persian Gulf line, it is between 15°S and 5°S, and has a mean transport of 13.4 Sv at about 93°E. On the Fremantle - Red Sea line, it is between 17°S and 3°S, and has a mean transport of 18.2 Sv at about 82°E. On the Reunion - Red Sea line, it is between 20°S and 7°S, and has a mean transport of 21 Sv at 55°E. These values are in good agreement with the SEC transport relative to 400 db estimated by HASTENRATH and GREISCHAR (1991), while reference to a deeper level gives considerably higher values in the range 33 to 39 Sv (WYRTKI, 1971; GODFREY and GOLDING, 1981). The deeper observations are larger than the model results of WOODBERRY et al. (1989) due to Indonesian throughflow (GODFREY and GOLDING, 1981). It is worth noting that the 400 db transport of the SEC increases from east to west (Fig 13) as a consequence of the Sverdrup transports generated by wind stress curl. The 400 m transports are not referenced to deep enough level to compare quantitatively to the Sverdrup transports (GODFREY, 1989).

Shipping Line	Latitude	Longitude	Mean Transport
Port Hedland-Japan	13°S - 9°S	123°E	5.5 Sv
Fremantle-Sunda	15°S - 7°S	106°E	9.2 Sv
Fremantle-Persian	15°S - 5°S	93°E	13.4 Sv
Fremantle-Red Sea	17°S - 3°S	82°E	18.2 Sv
La Reunion-Red Sea	20°S - 7°S	55°E	21 Sv

Table 1. Mean transport of the South Equatorial Current along the shipping lines of the Indian Ocean

The seasonal variation of the SEC transport was estimated along four shipping lines spanning the Indian Ocean (Fig 14). Only westward flow was counted in the monthly transports. The annual

cycle in the eastern Indian Ocean (Fremantle to Sunda Strait route) has a maximum westward transport of 17 Sv in August/September, at the time of maximum westward wind stress in the region. The transport has a distinct semiannual oscillation which MEYERS et al. (1993a) have associated with the reflection of the equatorial jets along the eastern boundary. A secondary maximum westward transport of 13 Sv is in January/February. In the central Indian Ocean (Fremantle to Persian Gulf route), there is a dominant annual cycle with the maximum in September/October (19 Sv) and the minimum in June/July (12 Sv). Further west (Fremantle to Red Sea route) the transport has a broad maximum from November to January (23 Sv) and a broad minimum between June and August (15 Sv). In the western Indian Ocean (Red Sea to Reunion route), the minimum is in April (18 Sv) and the maximum between October and December (26 Sv). The westward propagation of phase in maximum and minimum transport is associated with the annual Rossby wave in this region described by PERIGAUD AND DELECLUSE (1993).

Possible inconsistencies in the maps of transport (Fig's 6 and 7) were noted above. A careful inspection of the temperature sections on the XBT routes suggests that vertical shear and reference level velocities may in part be responsible for inconsistencies in 0 - 400 m transport. From 5°S to the equator, according to the isotherm pattern for February/March (Fig 15), there is spreading of the thermocline, similar to the Pacific Ocean, indicating westward transport at the surface and eastward transport below 100 m. On the Red Sea-Reunion and the Red Sea-Fremantle routes during January/February, transport is eastward on either side of the equator on the Reunion route and westward on the Fremantle route (Fig. 6). This inconsistency may be due to averaging vertically over the westward and eastward flows at different levels.

Conclusion:

Studies of the large scale oceanographic conditions in the Indian Ocean have been rare until the present time, due to lack of data. The French-Australian TOGA XBT network provides an opportunity to document the thermal, baroclinic variability. Seasonal variations have been first investigated on the basis of a preliminary climatology based on data collected during the first half of the TOGA Programme. While a climatology based on many

more observations will be possible at the end of TOGA, this first attempt has provided representative and quantitative measures of the transport of major currents, which previously were described qualitatively using surface drift data. The study has shown that in the western Indian Ocean currents and transports have a strong annual variation related to the monsoon regime. Interannual variations will be the subject of a further study.

Acknowledgements

Volunteer observers on merchant ships have generously collected the data in the field. Substantial external resources were provided by Royal Australian Navy, Department of the Environment (Australia), Bureau of Meteorology (Australia), NOAA (USA), Department of Education (Japan) and Japan Meteorological Agency. R.J. Bailey is the scientist-in-charge of the CSIRO Ocean Observing Networks. M. Prive is in charge of ORSTOM observations in Le Havre. A.P. Worby was the programmer for development of the climatology and L. Pigot calculated the EOF's. We gratefully acknowledge all of this support.

Captions

Figure 1: Surface dynamic height relative to 400 db in dynamic millimetres for January/February.

Figure 2: Surface dynamic height relative to 400 db in dynamic millimetres for August/September.

Figure 3: Surface dynamic height relative to 400 db in dynamic millimetres for April/May.

Figure 4: Eigenvector 1 and associated time function of the dynamic height relative to 400 db.

Figure 5: Eigenvector 2 and associated time function of the dynamic height relative to 400 db.

Figure 6: Transport in Sverdrups (10^6 m^3/s) relative to 400 db in January/February.

Figure 7: Transport in Sverdrups (10^6 m^3/s) relative to 400 db in August/September.

Figure 8: Transport in Sverdrups (10^6 m^3/s) in the Somali Current, 7.5° to 12.5°N, on the Reunion - Red Sea and Fremantle - Red Sea lines; transport between 7.5°N and 15.5°N on the Fremantle - Persian Gulf line.

Figure 9: Transport in Sverdrups (10^6 m^3/s) in the latitude band 2.5°N to 7.5°N.

Figure 10: Transport in Sverdrups (10^6 m^3/s) of the Equatorial Jet in the latitude band 0.5°S to 2.5°S.

Figure 11: Transport in Sverdrups (10^6 m^3/s) of the Equatorial Jet in the latitude band 0.5°N to 2.5°N.

Figure 12: Transport in Sverdrups (10^6 m^3/s) of the South Eqatorial Countercurrent (top) and latitude of the Countercurrent trough (bottom).

Figure 13: Increase of the SEC transport from the east to the west and of the 20°C isotherm depths at the southern boundary of the current.

Figure 14: Annual regime of the South Equatorial Current transport along four routes in the tropical Indian Ocean. The variation of transports in Sverdrups are represented clockwise, with the value for the January/February mean at noon, for April/May at 3 o'clock, etc. The annual maximum transport on each route is indicated by a dot.

Figure 15: Vertical isotherms distribution 0-500 m and 0° - 20°S along the routes Red Sea-Reunion and Red Sea-Fremantle route for February/March.

References

COLBORN, J. G. (1975). *The thermal Structure of the Indian Ocean.* Univ. of Hawaii Press, Honolulu, 173 pp.

DONGUY, J. R.(1974). Une annee d'observations de surface dans la zone de monsson de la partie occidentale de l'Ocean Indien *Cah. ORSTOM. Ser. Oceanog.*,**12**, 2, 177-128.

DONGUY, J. R. and B. PITON (1991). The Mozambique Channel revisited. *Oceanol. Acta*, **15**, 549-558.

DONGUY, J. R. and G. MEYERS (1992). Zonal surfaces current distribution in the tropical Indian Ocean from XBT TOGA network. *TOGA Notes,* July 1992, 7-11.

DUING, W., R. L. MOLINARI and J. C. SWALLOW (1980). Somali Current: evolution of surface flow. *Science*, **209**, 588-590.

GODFREY, J. S. (1989). A Sverdrup model of the depth integrated flow for the world ocean allowing for island circulations. *Geophys. Astrophys. Fluid Dynamics,* **45**, 89-112.

GODFREY, J. S. and T. J. GOLDING (1981). The Sverdrup relation in the Indian Ocean and the effect of Pacific-Indian circulation and on the East Australian Current. *J. Phys. Oceanogr.*, **11**, 771-779.

HASTENRATH, S. and L. GREISCHAR (1991). The monsoonal current regimes of the Tropical Indian Ocean. Observed surface flow fields and their geostrophic and wind-driven components. *J. Geophys. Res.,* **96**, 12619-12633.

KNOX, R. A. (1987). The Indian Ocean: Interaction with the Monsoon. IN: *Monsoons,* ed's J.S. Fein and P.L. Stephens, John Wiley & Sons, New York, pp 365-397.

LEVITUS, S (1982). Climatological Atlas of the World Ocean NOAA. Professional Paper No. 13, US Department of Commerce.

MEYERS, G. (1979). On the annual Rossby wave in the tropical North Pacific Ocean. *J. Phys. Oceanogr.* **9**, 663-674.

MEYERS, G. (1992). Indian Ocean Analyses. IN: *Proceedings of the Ocean Climate Data Workshop.* Goddard Space Flight Center, Greenbelt, pp 109-129..

MEYERS, G., R. J. BAILEY and A. P. WORBY (1993a). Volume transport of the Indonesian throughflow relative to 400 db. *Science* (submitted)

MEYERS, G., R. J. BAILEY and A. P. WORBY (1993b). *Working Atlas of Thermal Structure on TOGA XBT lines in the Indian Ocean.* CSIRO Marine Laboratories Report xxx (in preparation).

MOLINARI, R. L., D. OLSON and G. REVERDIN (1990). Surface current distributions in the Tropical Indian Ocean derived from compilations of surface buoy trajectories. *J. Geophys. Res.*, **95**, 7217-7238.

PERIGAUD, C. and P. DELECLUSE (1993). Annual sea level variations in the southeastern tropical Indian Ocean. *J. Geophys. Res.*, **97**, 20169-20178.

SCHOTT, F., M. FIEUX, J. KINDLE, J. SWALLOW and R. ZANTOPP (1988). The boundary currents east and north of Madagascar, 2. Direct measurements and model comparisons. *J. Geophys. Res.*, **93**, 4963-4974.

SWALLOW, J. C. and M. FIEUX (1982). Historical evidence for two gyres in the Somali Current. *J. Mar. Res* , **40**, Suppl 747-755.

SWALLOW, J. C., M. FIEUX AND F. SCHOTT (1988). The boundary currents east and north of Madagascar, 1. Geostrophic currents and transports. *J. Geophys. Res.*, **93**, 4951-4962.

SWALLOW, J. C., F. SCHOTT and M. FIEUX (1991). Structure and transport of the East Arican Coastal Current. *J. Geophys Res*, **96**, 22245-22257.

WOODBERRY, K. E., M. E. LUTHER and J. O'BRIEN (1989). The wind-driven seasonal circulation in the Southern Tropical Indian Ocean *J. Geophys Res.*, **94**, 17985-18002.

WYRTKI, K. (1971). Oceanographic Atlas of the International Indian Ocean Expedition, 531 pp. National Science Foundation, Washington DC.

WYRTKI, K. (1973a). Physical Oceanography of the Indian Ocean. In: Ecological Studies - Analysis and Synthesis. Vol. 3 edited by B. Zeitzchel Springer-Verlag, Berlin: 18-36.

WYRTKI, K. (1973b). An equatorial jet in the Indian Ocean *Science*, **181**, 262-264.

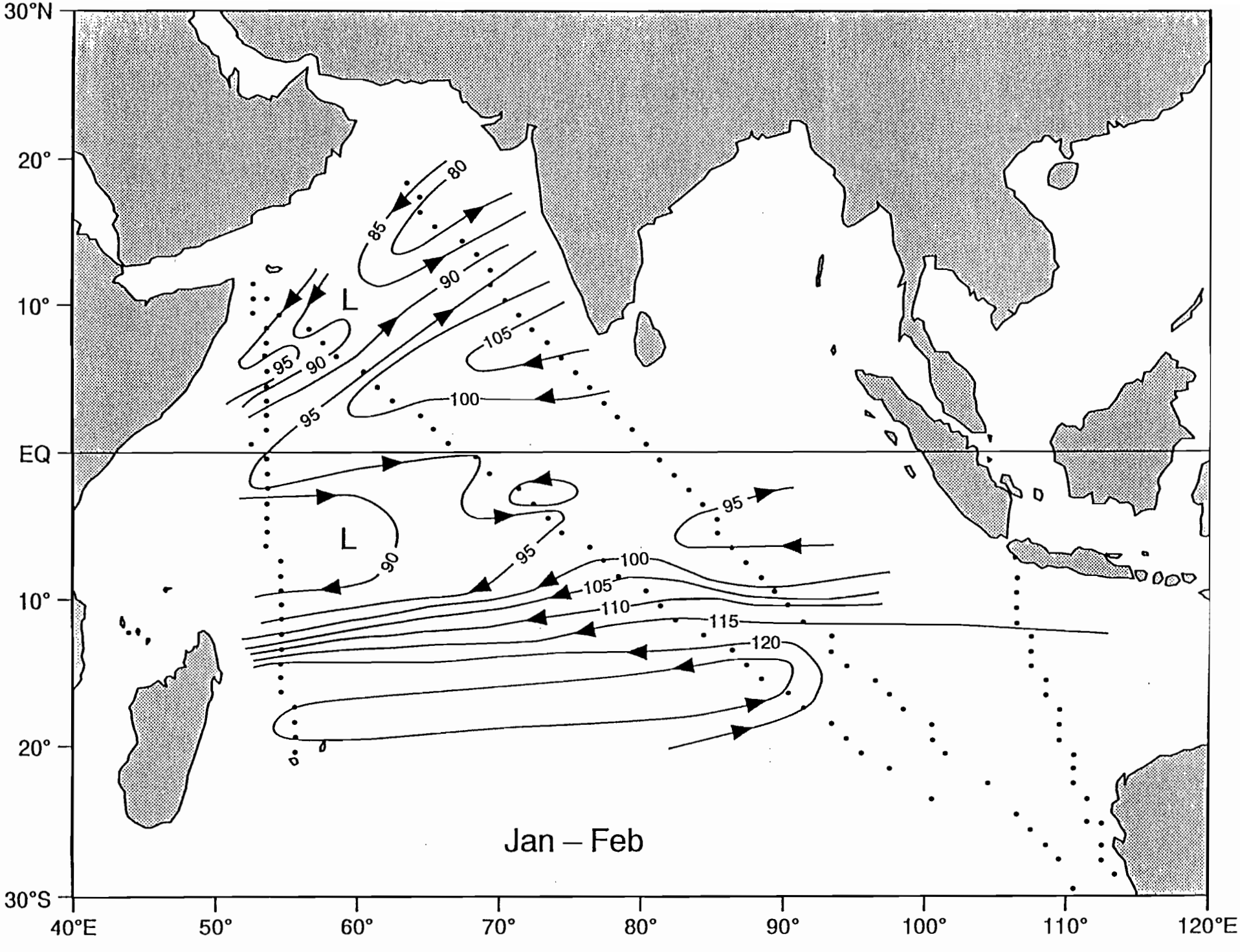

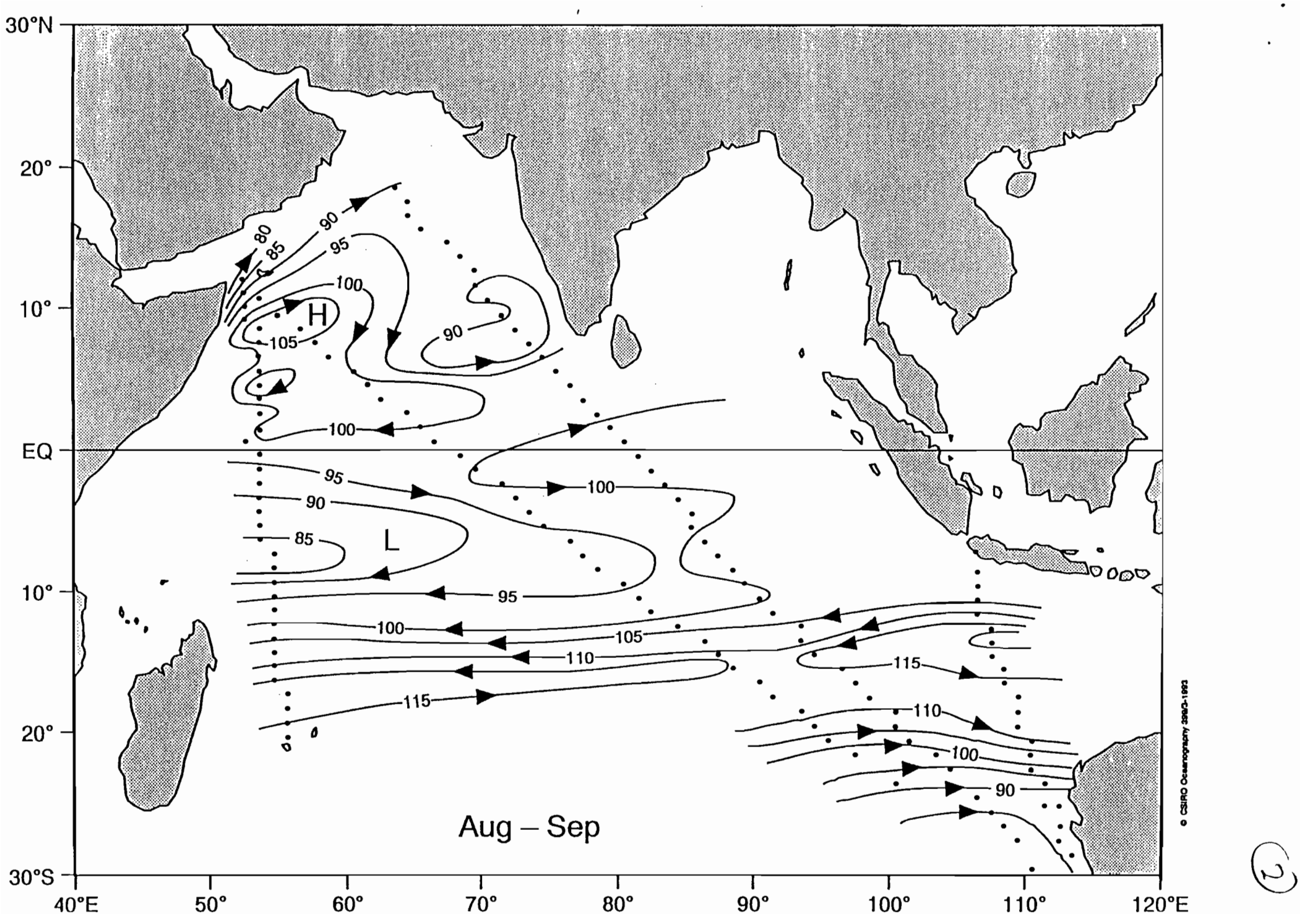
30°N
20°
10°
EQ
10°
20°
30°S
40°E
50°
60°
70°
80°
90°
100°
110°
120°E
H
L
80
85
90
95
100
105
110
115
Aug – Sep
© CSIRO Oceanography 1992-1993

(2)

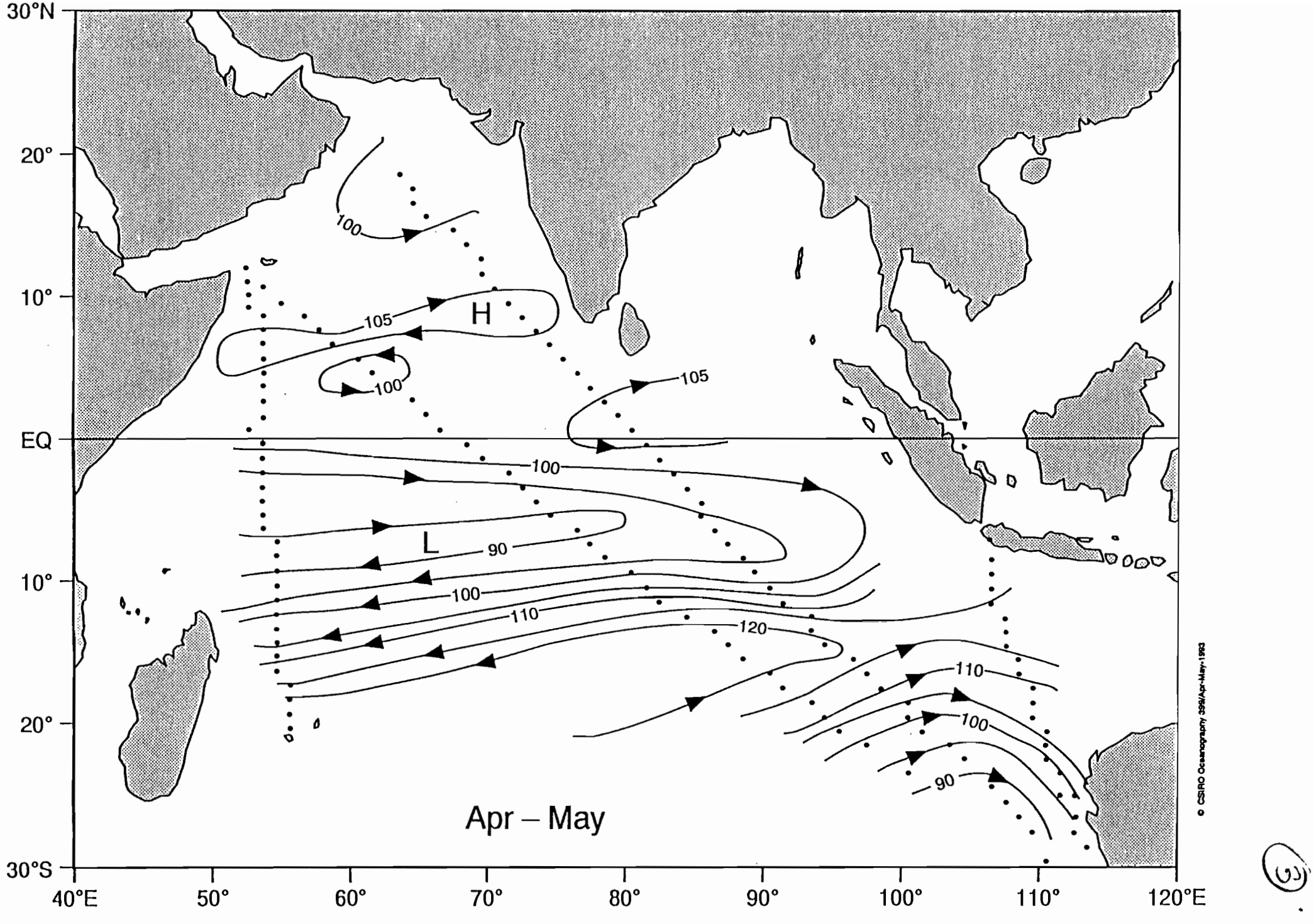
30°N
20°
10°
EQ
10°
20°
30°S
40°E
50°
60°
70°
80°
90°
100°
110°
120°E
H
L
100
105
100
105
100
90
100
110
120
110
100
90
Apr – May
© CSIRO Oceanography 396/Apr-May-1993

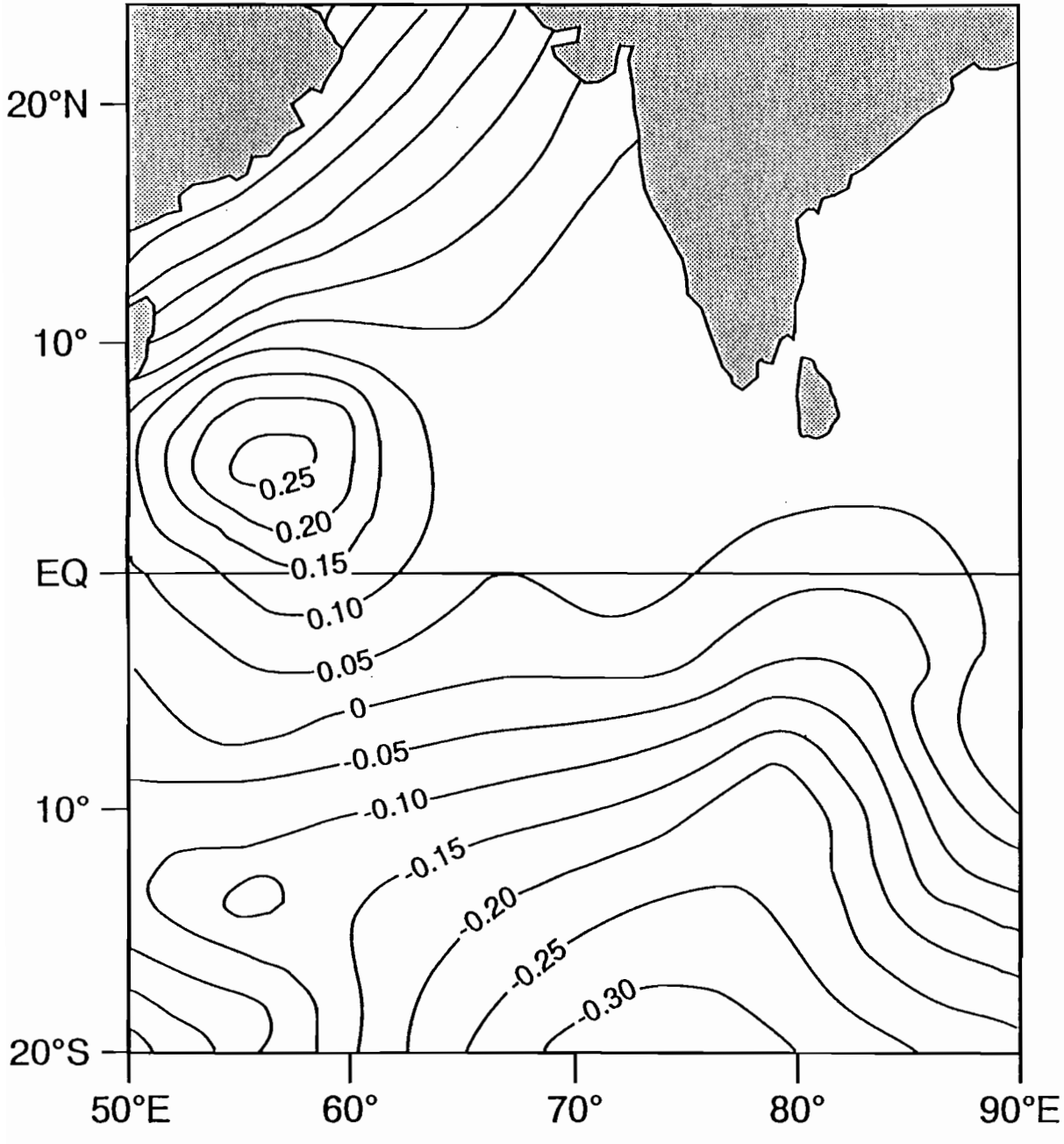

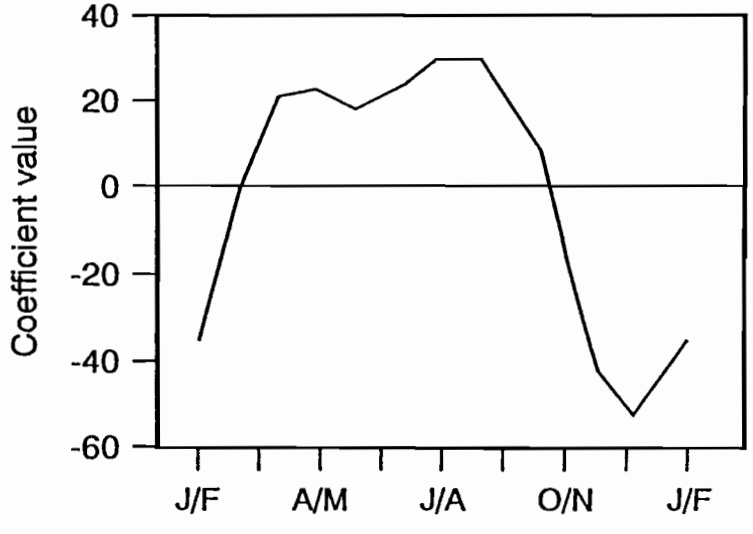

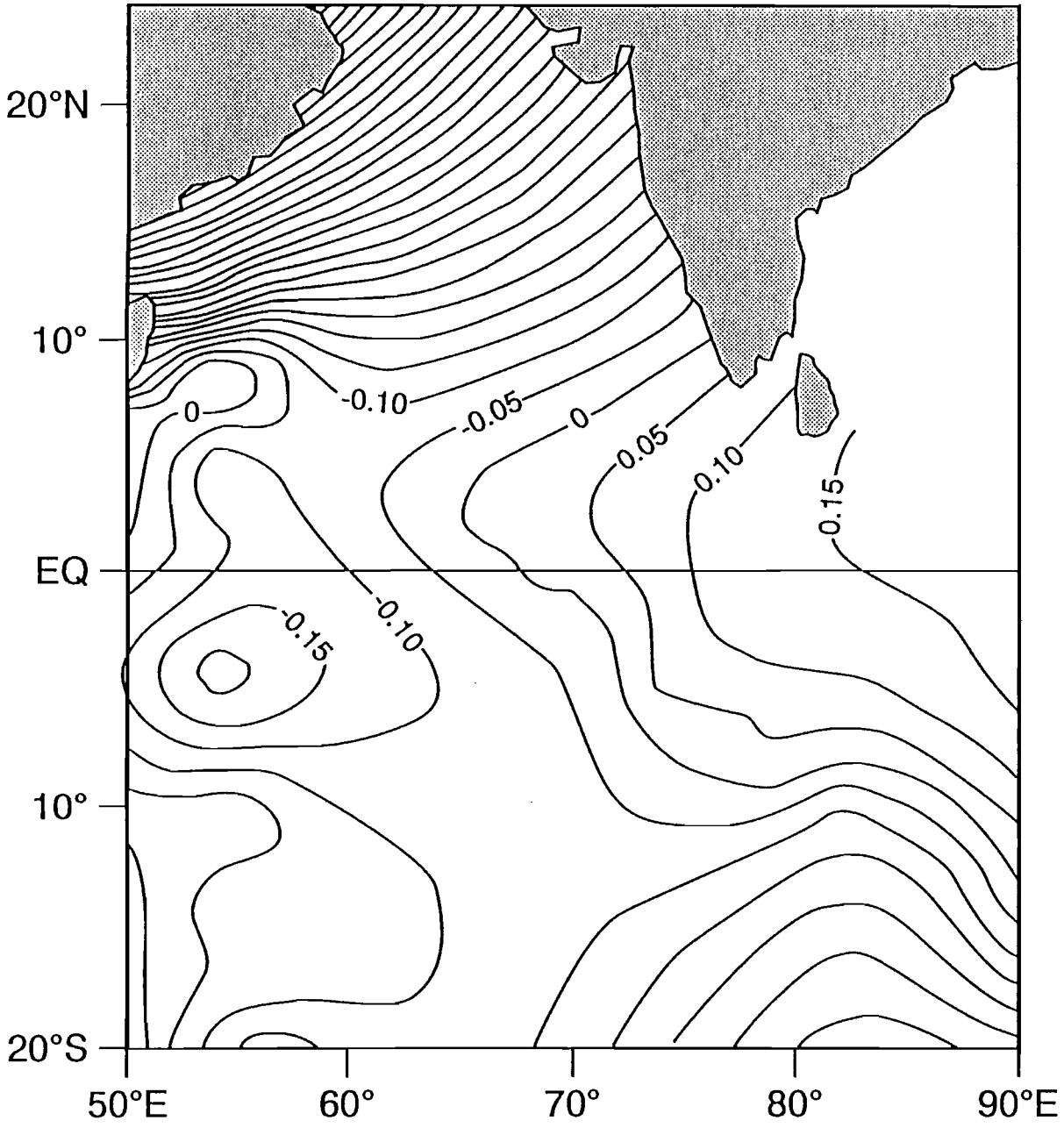

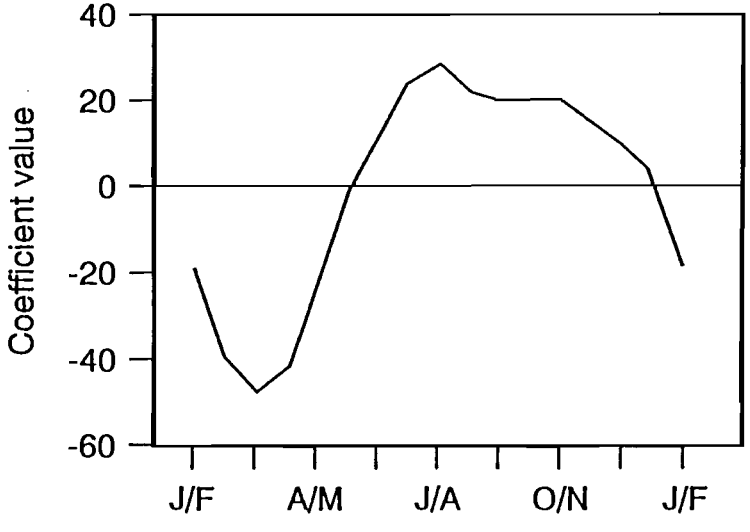

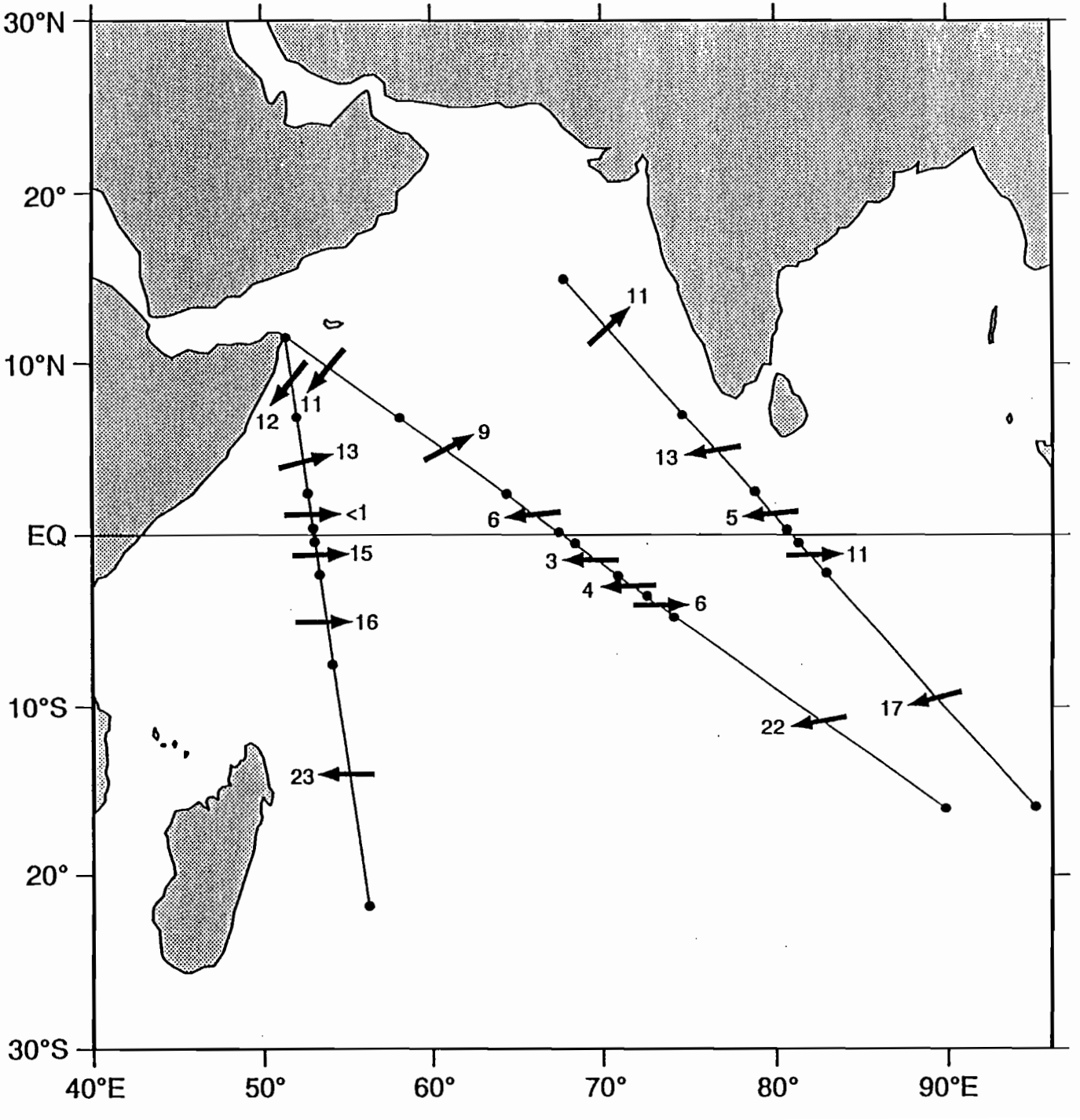
30°N
20°
10°N
EQ
10°S
20°
30°S
40°E
50°
60°
70°
80°
90°E
11
12
11
13
<1
15
16
23
9
6
3
4
6
11
13
5
11
17
22

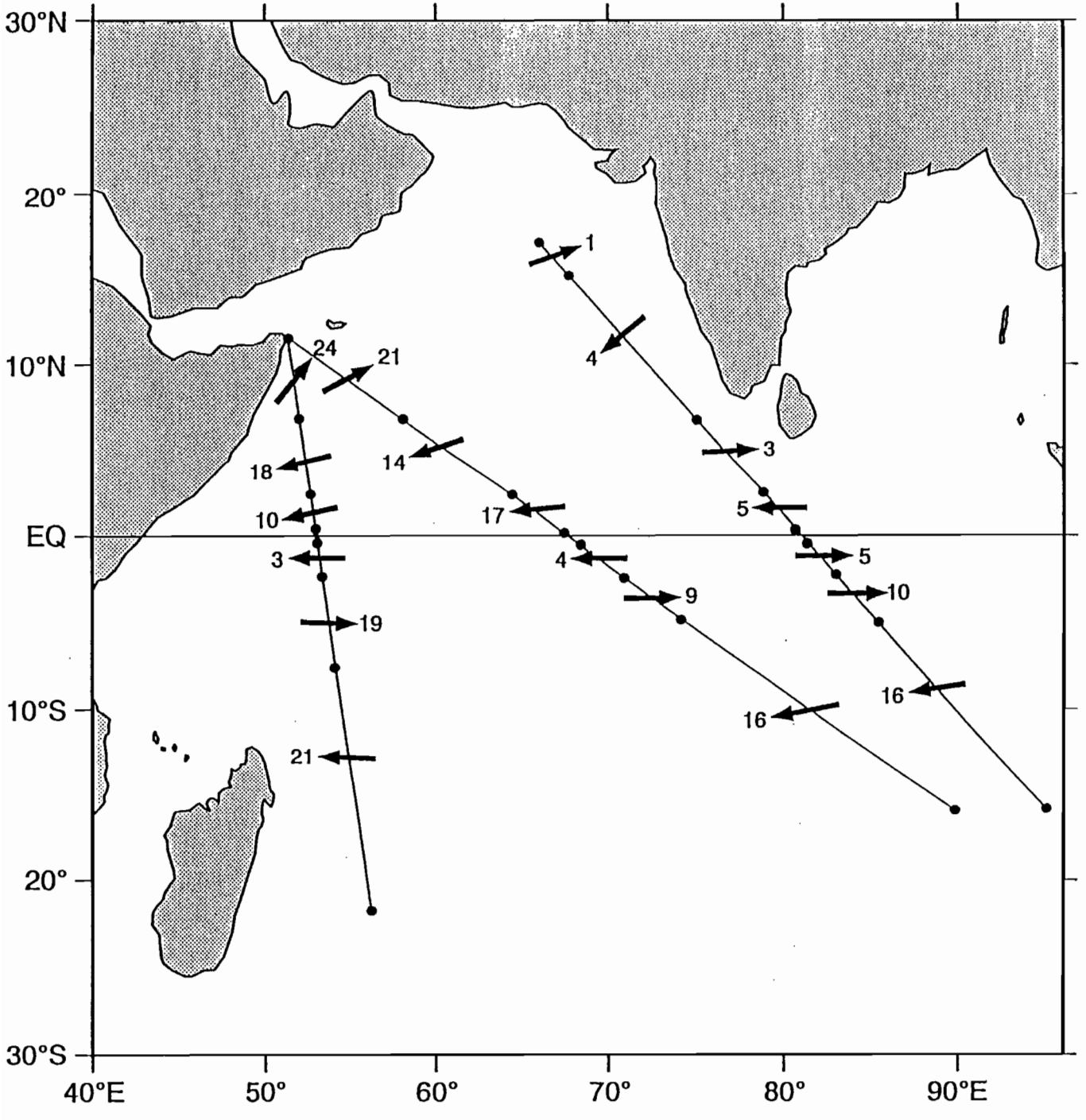

7

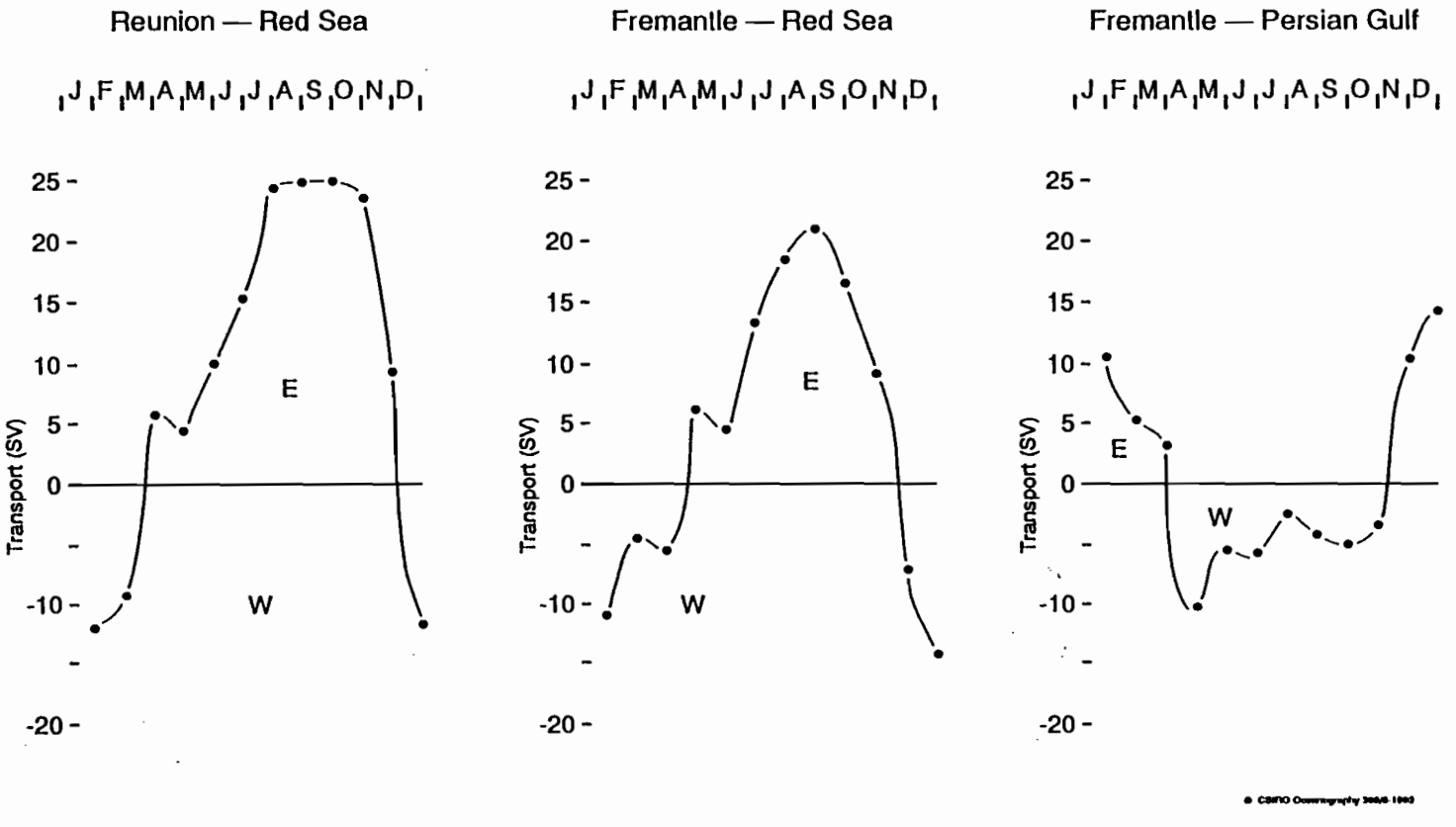

Reunion — Red Sea

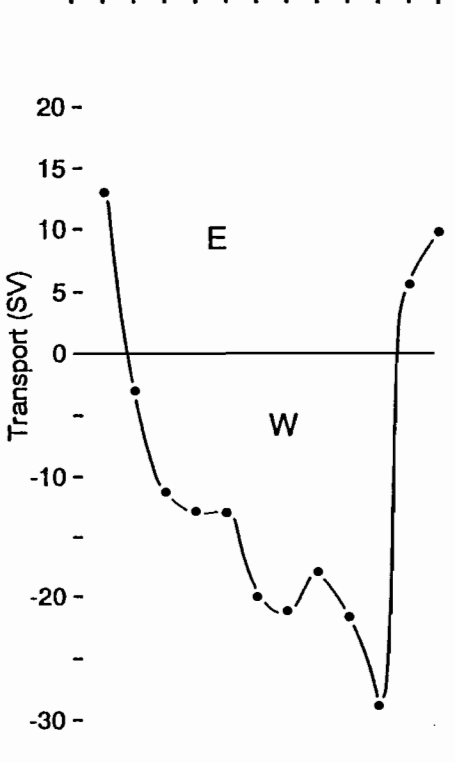

Fremantle — Red Sea

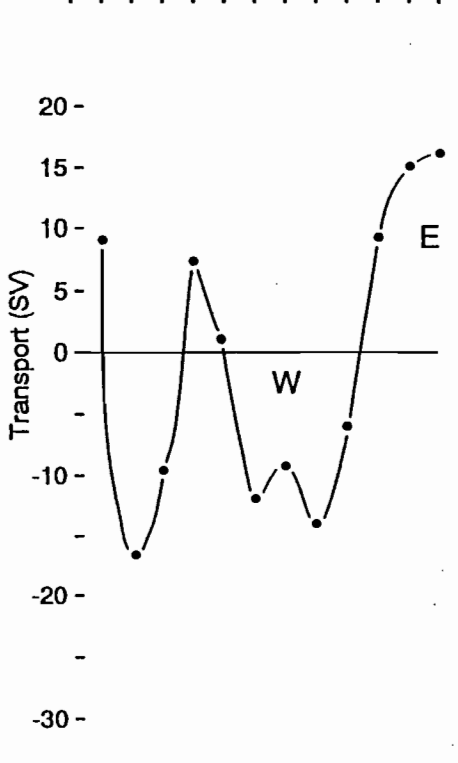

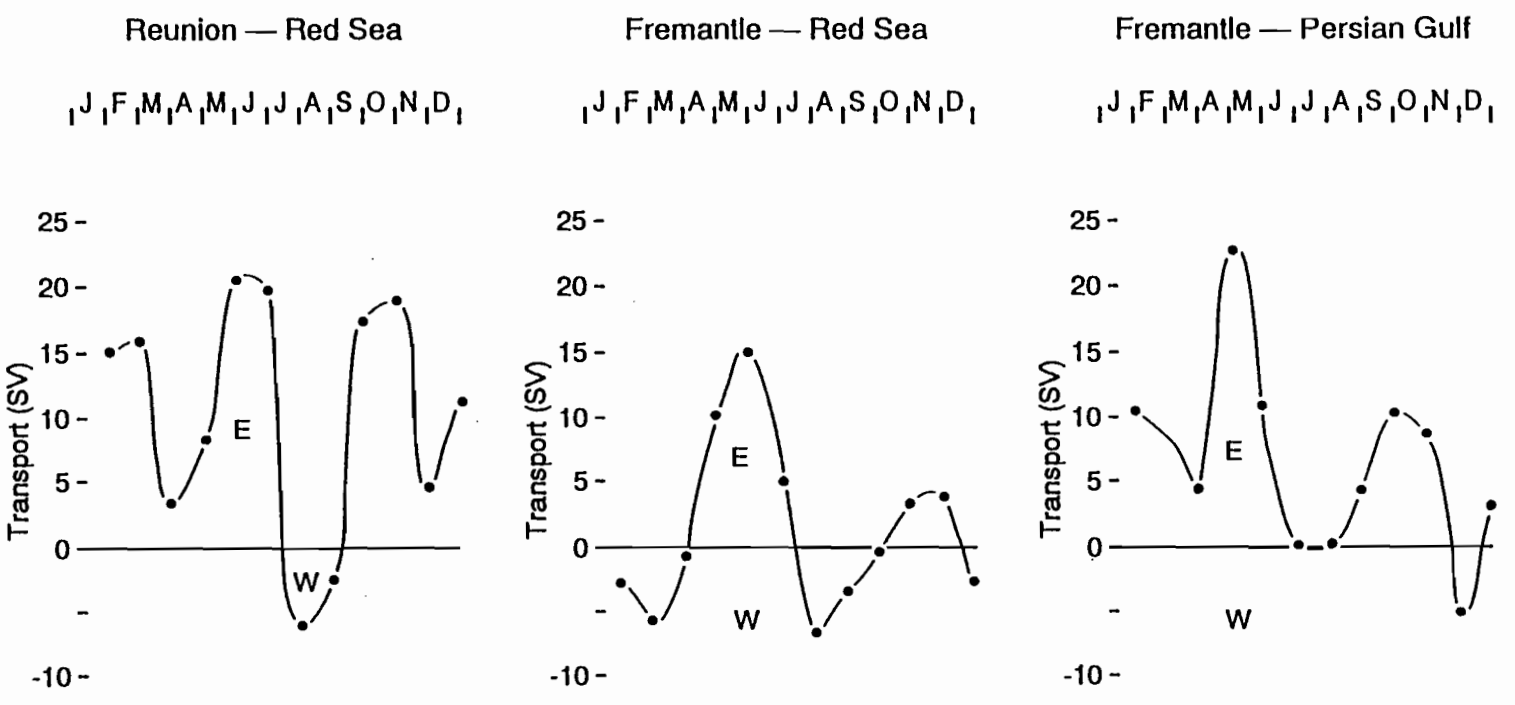

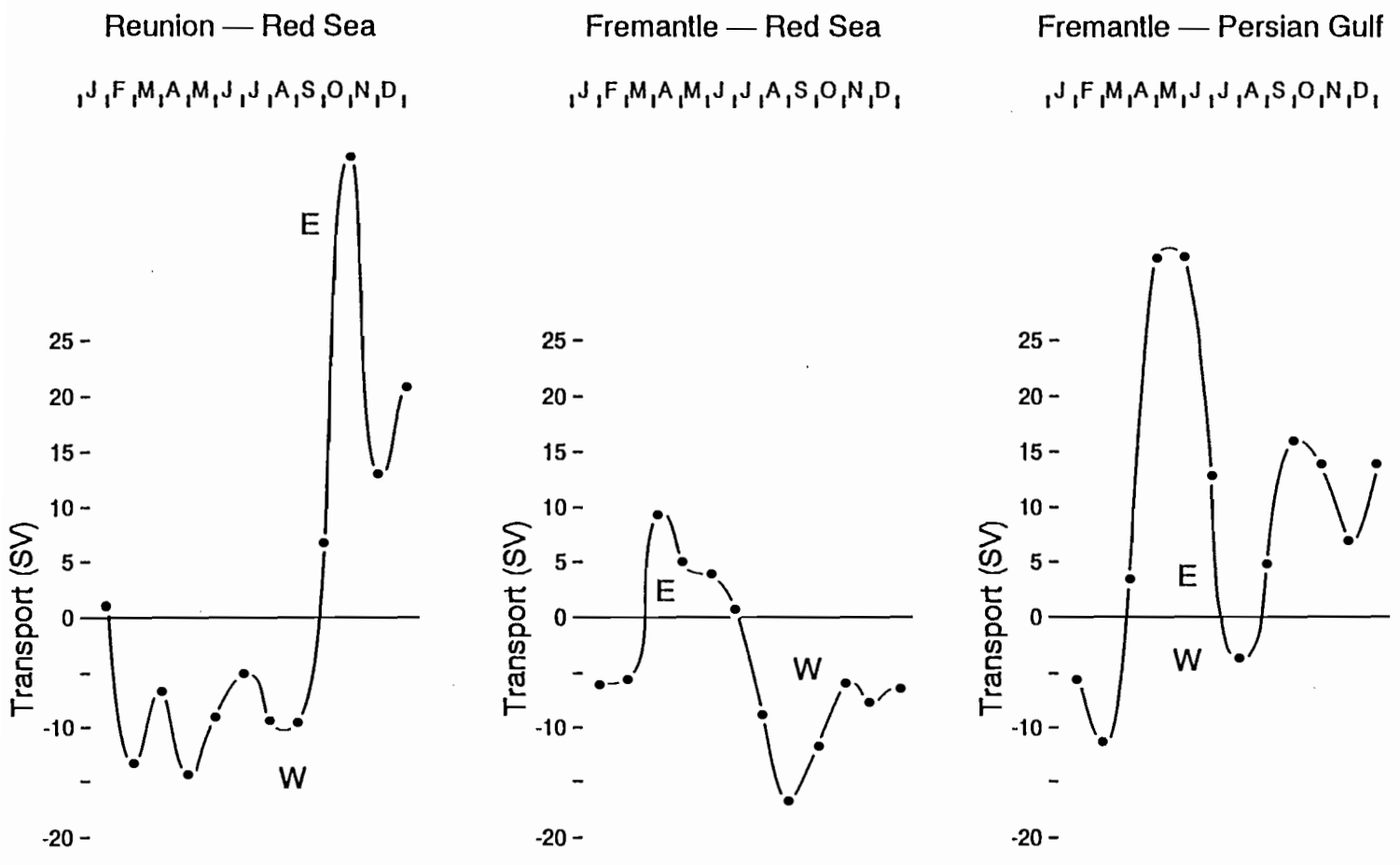
Reunion — Red Sea
J F M A M J J A S O N D
Transport (SV)
25
20
15
10
5
0
-10
-20
E
W
Fremantle — Red Sea
J F M A M J J A S O N D
Transport (SV)
25
20
15
10
5
0
-10
-20
E
W
Fremantle — Persian Gulf
J F M A M J J A S O N D
Transport (SV)
25
20
15
10
5
0
-10
-20
E
W

South Equatorial Counter Current

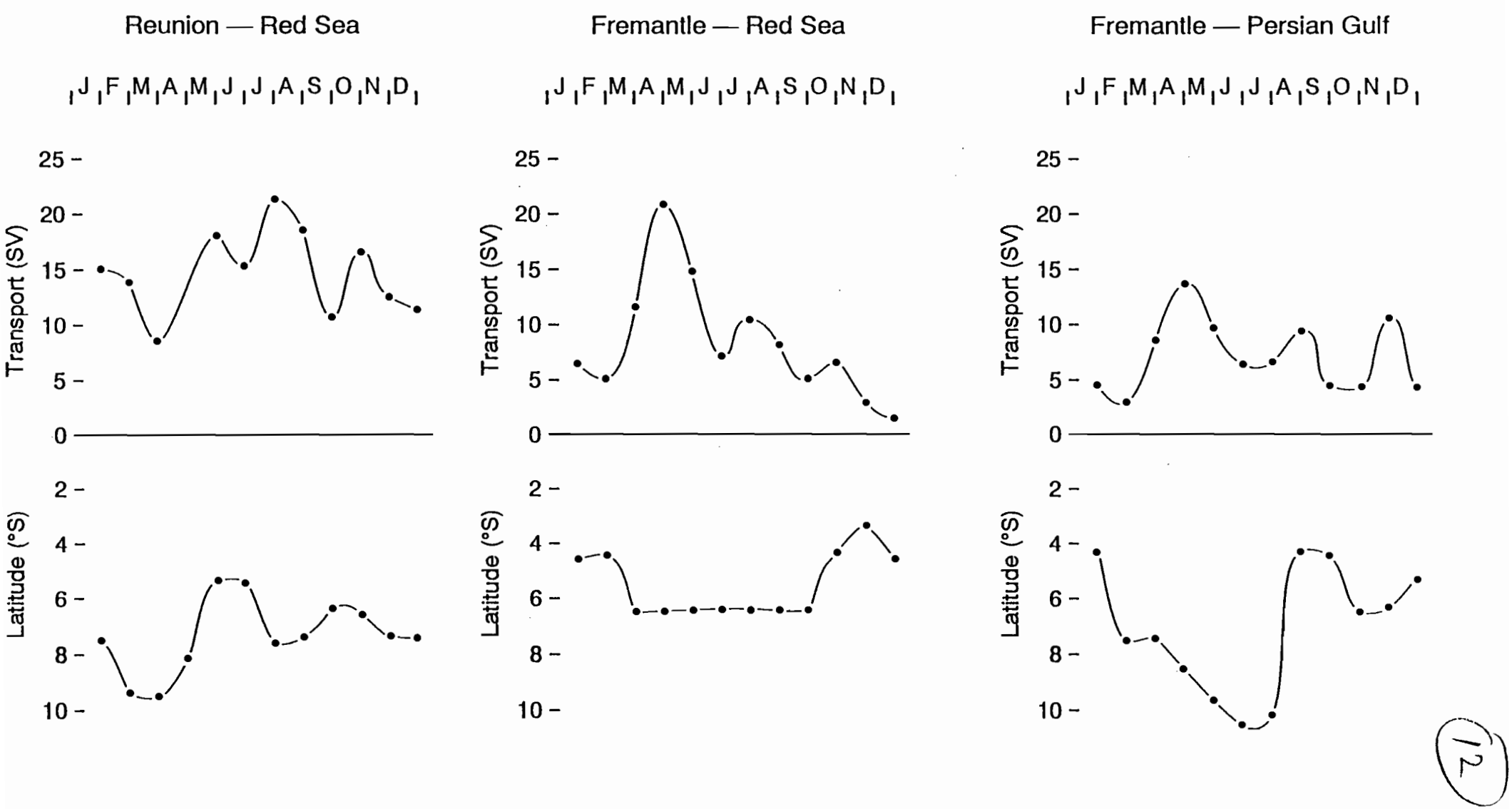

12

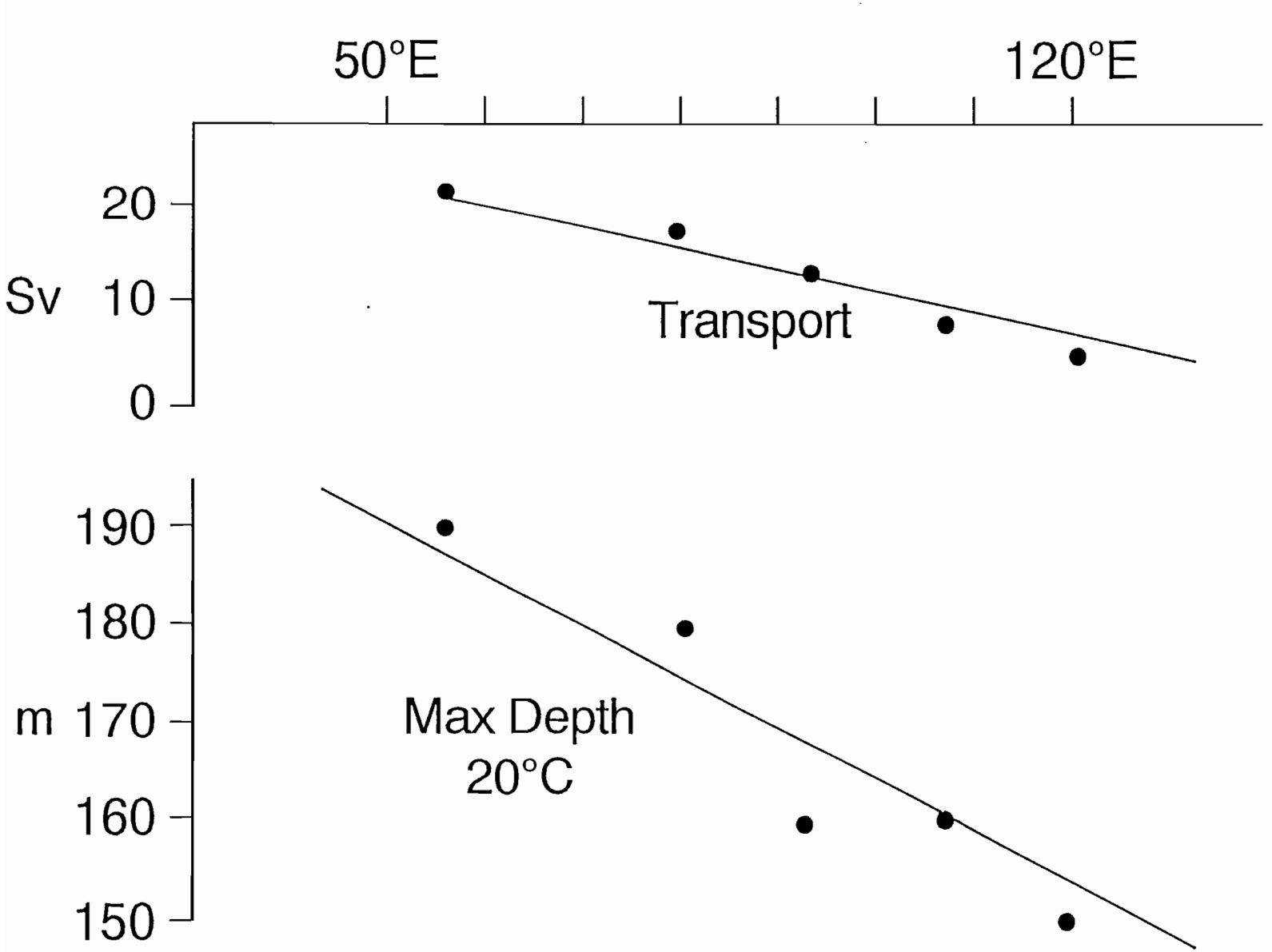

13.

SOUTH EQUATORIAL CURRENT

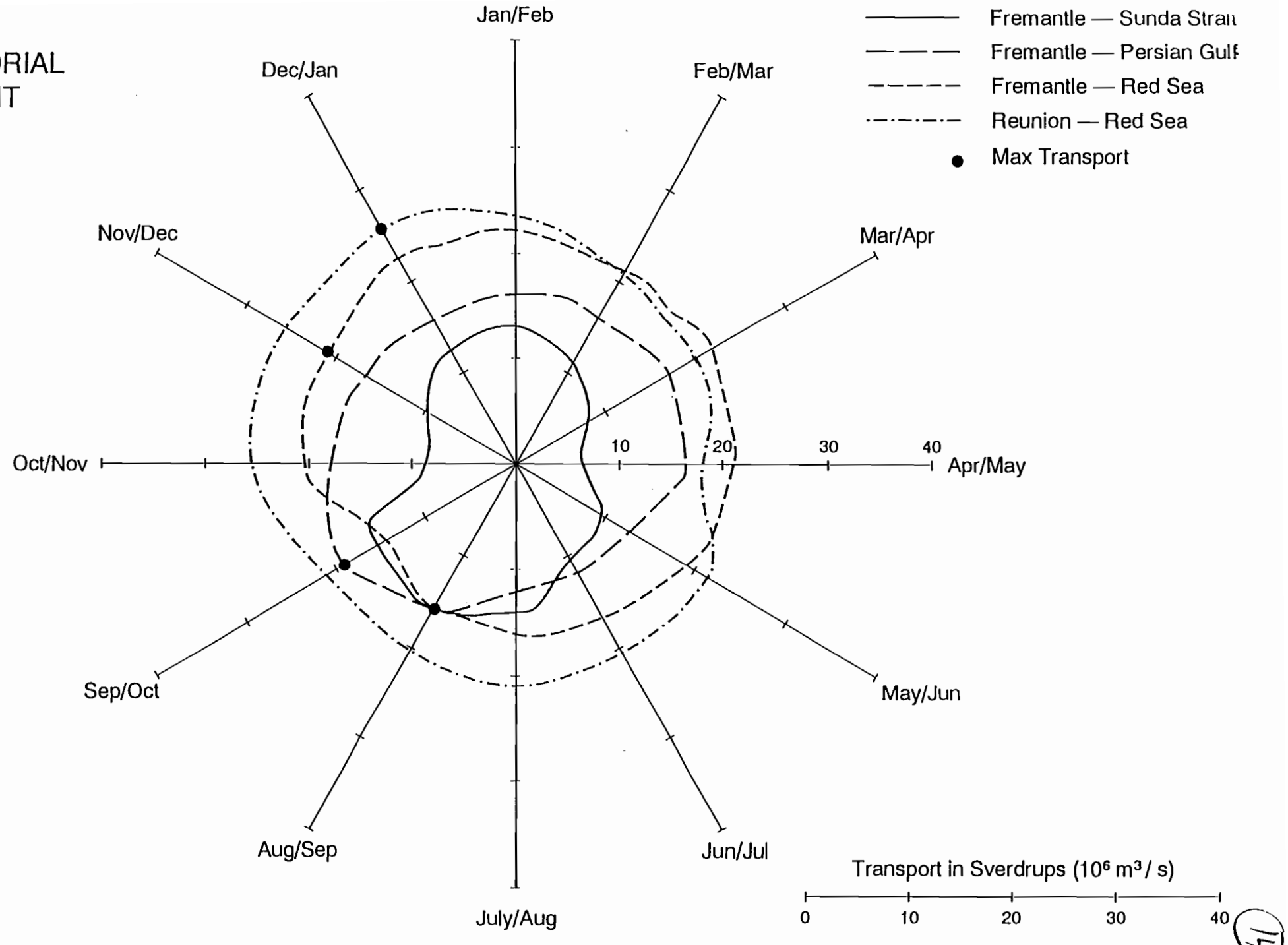

Reunion Island — Red Sea

Mean Temperature

Jan 1985 — Jun 1989

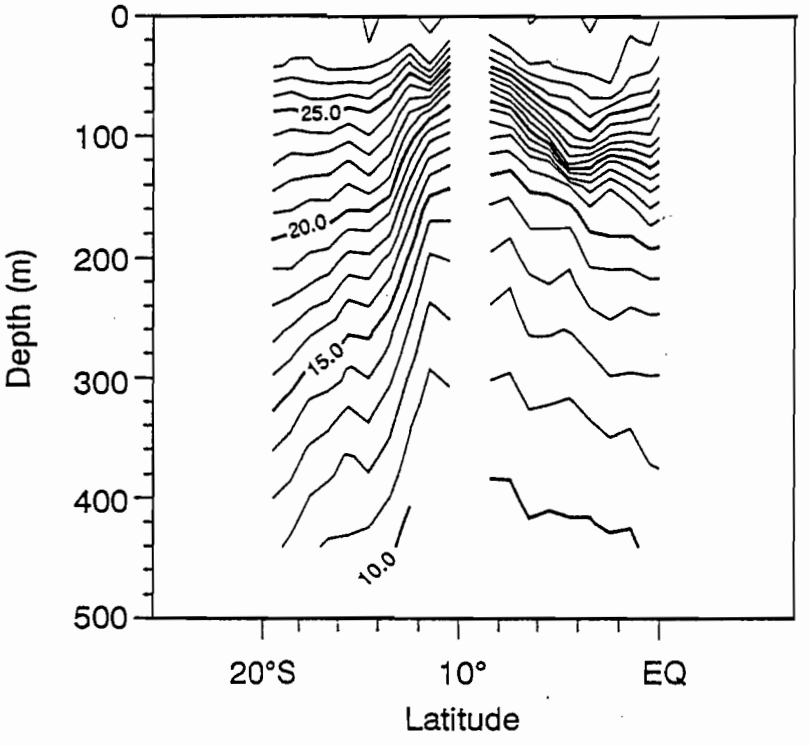

Fremantle — Red Sea

Mean Temperature

Aug 1986 — Aug 1989

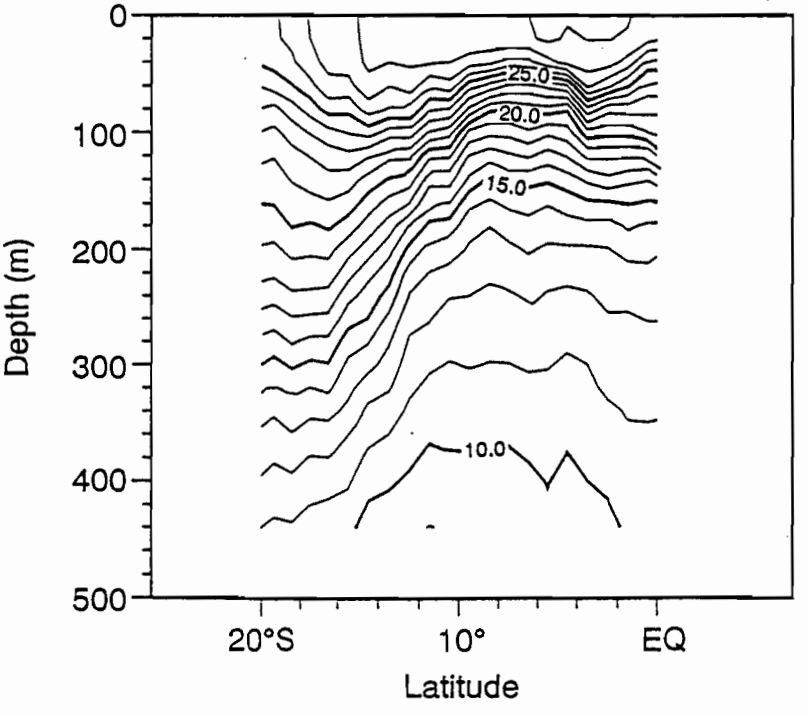

VOLUME TRANSPORT OF INDONESIAN THROUGHFLOW

G. Meyers*, R. J. Bailey
CSIRO Division of Oceanography
GPO Box 1538
Hobart TAS 7001 Australia

and

A. P. Worby
IASOS, University of Tasmania
GPO Box 252C
Hobart TAS 7005 Australia

10 August 1993

The Indonesian throughflow, a current of upper ocean waters from the Pacific to the Indian Ocean[1], has been measured in the upper 400 m during a six year period, permitting estimates of the mean and mean annual cycle of volume transport. The mean transport is found to be 5 x 10^6 m^3/s relative to 400 m, and the transport due to reference velocity at 400 m determined from climatological data is 6 x 10^6 m^3/s, giving a total upper 400 m transport of 11 x 10^6 m^3/s. Using the same reference velocity, the annual maximum throughflow entering the Indian Ocean is 18 x 10^6 m^3/s in August-September.

Estimation of the mean transport from past observational studies was not possible due in part to the variety of indirect methods that were used, and in part to temporal and spatial variability of throughflow[2] which was not resolved in sampling. The throughflow is recognized as a major component of global scale interchange of water masses between ocean basins and as such improved documentation of its magnitude is needed for research on a wide range of subjects including oceanic heat and salt budgets, climate change, geochemistry and paleo-oceanography. The project reported here was started in 1983 and was the first to collect routine, systematic observations of the thermal (baroclinic) structure of throughflow.

Temperature sections were observed by expendable bathythermograph (XBT) to a depth of 400 m using volunteer observing ships on the merchant shipping routes (Fig. 1) Shark Bay–Sunda Strait (Section A), Port Hedland–Japan (Section B) and Jakarta–Torres Strait (Section C)[3]. The XBT profiles were obtained at approximately every 100 km along the routes. The number of transects collected during the six years was 105, 95 and 56 on sections A, B and C, respectively. Mean temperature sections were prepared for each bimonth (January-February, February-March, etc.), on a spatial grid of 1° latitude or longitude along the routes, except that special bins were used for waters less than 1000 m depth off Shark Bay, and for all drops north of 8°S off Sunda Strait. The mean temperatures were used to calculate dynamic height, geostrophic currents and volume transports (relative to 400 m), using the annual mean temperature/salinity relationship[4]. The data processing and the annual temperature variations are described in more detail in a report[5].

The long term annual mean temperature sections show the horizontal gradients associated with baroclinic currents. The thermocline slopes upward from Shark Bay to Sunda Strait (Fig. 2A) indicating net transport toward the west. North of Port Hedland, a ridge in the thermocline at 8.5 °S (Fig. 2B). indicates eastward flow on the northern side of the Indonesian Archipelago and westward flow on the southern side. The zonal section across the Flores and Banda Seas (Fig. 2C) indicates southward flow in Makassar Strait, and southward flow again between Alor and the Arafura Shelf.

The bimonthly, net transport functions relative to 400 m were calculated for each section and the results averaged to produce the annual mean pattern of circulation (Fig. 3). Volume transports in 10^6 m^3/s (or Sverdrups, Sv) are indicated for segments of each track indicated by dots. The mean relative throughflow is 5 to 6 Sv

flowing southward in Makassar Strait, then eastward along the northern side of the Indonesian Archipelago, then southward again through the passages on either side of Timor, and finally westward. The throughflow joins the eastern gyral current (EGC), an extension of the subtropical gyre into the region between Australia and Indonesia, to form the South Equatorial Current (SEC) south of Java. The trajectory of throughflow inferred from XBT data is in good agreement with the earlier studies[1], particularly the Snellius Expedition. The net westward transport across section A (5.2 Sv) is in good agreement with the net southward transport across section C (4.9 Sv, made up of 5.4 Sv southward minus 5.2 Sv eastward plus 4.7 Sv southward.)

The climatological hydrographic data of Levitus[4] was used to assess the effect of a non-zero reference velocity at 400 m. The 400 m relative transport from Levitus was in excellent agreement with the XBT transport on section A, except that the Leeuwin Current (LC) did not appear in the Levitus data. The sill depths in the Indonesian Seas are closer to 1500 m. Calculation of the transport in the upper 400 m relative to 1500 m using Levitus data indicated that the reference velocity at 400 m integrated vertically to the surface gives an additional 6 Sv in the upper 400 m. The combined transports of relative and reference currents gives 11 Sv for throughflow in the upper 400 m.

Variability of throughflow over a range of scales from mesoscale to regional and seasonal has been suggested by observational[2] and modelling[6] studies. The annual variation was qualitatively described[7] using the difference in sea level between Darwin and Davao (Mindanao), which indicated that the driving force for throughflow, the pressure gradient between the Pacific and the Indian Oceans, is greatest during July to September.

The variation of transport observed on section A (Fig. 4, top panel) is generally in agreement with this description. The transports of the SEC and EGC are largest in August-September. The South Java Current (SJC) is an eastward flow observed on the northern end of the section during March–July and October–November, within 200 km of the coast. The semiannual maxima of SJC are also prominent in models of the region[6]. When the SJC disappears during August–September and December–February, the SEC spreads northward to the coast of Java. The maximum eastward transport of the SJC is 6 Sv in May/June, which may not be in phase with the salinity driven surface current[2]. The southward LC has no apparent seasonal variation at this latitude.

The net relative transport through section A (Fig. 4, middle panel, solid line) varies from a maximum of 12 Sv westward in August/September to nil in May/June and October/November. Taking account of the upper layer transport associated with the reference velocity at 400 m (6 Sv, discussed above), the maximum is 18 Sv, in good agreement with the recent detailed hydrographic section by Fieux et al.[2].

The variations are related dynamically to the Monsoon winds. The maximum westward transport occurs in the season when the westward wind stress over the

section is strongest, namely during the austral winter Monsoon. The directly wind-driven (Ekman) transport shifts surface waters to the southern side of the section and depletes them on the northern side, increasing the upward slope of the thermocline between Australia and Java and the geostrophic flow[8]. The minima of westward transport occur when the eastward SJC strengthens and cancels the westward flow of SEC. The eastward flow is in part generated by the local windstress along the coasts of Sumatra and Java during January to March and in part it is the eastern boundary reflection of the semiannual eastward, equatorial jets generated in the central Indian Ocean during the Monsoon transitions[6,9].

The annual variation of net southward transport on section C (Fig. 4, middle panel, dashed line) is not in phase with the westward transport on section A. While this result is surprising at first, the variations on segments of section C (not presented) -- southward flow south of Makassar Strait; eastward flow on the northern side of Flores I.; and southward flow between Alor I. and the Arafura Shelf — suggest a reasonable dynamics. Transports southward and eastward on all three segments increase during January to May. The increase of southward transport south of Makassar Strait is markedly the strongest of the three in this season, indicating that some of the water must leave the Flores Sea through Lombok Strait[10]. The three currents all relax rapidly in June, with the onset of the opposite Monsoon. However, the eastward flow north of Flores I. and the southward flow near Timor soon begin to increase again, reaching a secondary peak during August–November. The peak-flow must be the response to the Pacific to Indian Ocean pressure gradient. The August peak does not appear strongly south of Makassar Strait, probably because the Makassar waters are swept into the shallow Java Sea by Monsoon winds in this season. Thus the August peak in flow between Alor I and the Arafura Shelf implies water leaving the Pacific Ocean through the Molucca and Halmahera Seas in austral winter, which is consistent with the fine scale model by Inoue and Welsh[6].

The net southward transport on section C exceeds the westward transport on section A (Fig. 4, middle panel) during March–June, reaching a maximum of 10 Sv in May/June when the westward transport is nil. Thus an inflow of upper layer water builds up in the region south of Indonesia during this season. The westward transport exceeds the southward during most of the rest of the year, as the throughflow leaves the region and joins the circulation of the Indian Ocean. The inference is that throughflow does not accelerate and decelerate uniformly all along its trajectory during the seasonal cycle and the region between Australia and Indonesia acts as a buffer to accomodate the currents with differing phases. The region south of Java was also described as a buffer by Quadfasal and Cresswell[2]. It is important to note that the buffer is fed by currents from the Indian Ocean as well as the Pacific[11]. The depth of the 20° C isotherm averaged over the two meridional sections between Australia and Indonesia increases as the buffer fills during March thru June (Fig. 4, bottom) and rises during most of the rest of the year while the buffer empties into the Indian Ocean.

The description of Indonesian throughflow on section A presented here was compared in a related study[8] to results of the seasonally forced Semtner and Chervin model[6] and we found a close correspondence between the observed and modelled temperature sections and transports. While this increases confidence in the description, the results are preliminary because the sampling program is still in progress. Sampling will continue atleast until 1995, when it will be possible to calculate more robust averages with temperature sections to a depth of 750 m.

References

1. Wyrtki, K. (1957) *Proc. 9th Pacific Sci. Congr.* **16**, 61-66; Postma, H. (1958) *The Snellius Expedition*. Vol. II, Part 8, 116 pp; Godfrey, J. S. and Golding, T. J. (1981) *J. Phys. Oceanogr.* **11**, 771-779. Gordon, A (1986) *J. Geophys. Res.*. **91**, 5037-5046; Broecker, W.S. (1991) *Oceanography* **4**, 79-89.

2. Quadfasel, D. and G.R. Cresswell (1992) *J. Geophys. Res.*, **97**, 3685-3688; Fieux, M. et al. (1993) *Deep Sea Res.* (in press); Cresswell et al. (1993) *J. Geophys. Res.*, (in press). Quadfasal and Cresswell discuss the influence of salinity gradients on the South Java Current. A near surface (<50 m) baroclinic coastal jet develops within this current due to high rainfall and river-runoff during December -- February. Their description of the variations of the surface current is different from our Fig 4 because: a) seasonal variations of salinity are not included in our study; b) transports were estimated in the upper 400 m in contrast to upper 50 m currents; and c) westward transport on the Java coast was included in the South Equatorial Current in this study.

3. Since 1985 the sampling program has operated under auspices of the International Tropical Ocean Global Atmosphere Program (TOGA) and since 1990 under auspices of the World Ocean Circulation Experiment (WOCE). The temperature profiles were measured to 450 m depth during 1983-1986 on sections A and C and to 750 m depth on sections A, B and C since 1987. The sampling program will continue at least until the end of TOGA (1995), and possibly longer under auspices of the Global Ocean Observing System.

4. Levitus, S. (1982) *Climatological Atlas of the World Ocean* NOAA Prof. Pap. 13, 173 pp. The annual mean salinity was used so that the calculated currents and transports would be representative of temperature changes observed by XBT. Neglecting the annual variations of surface salinity introduces an error in our transport measurements of about 1 Sv. The salinity gradients associated with baroclinic throughflow have been discussed recently[2,6].

5. Meyers, G., R.J. Bailey and A.P. Worby (1993) *Working Atlas of Thermal Structure on the TOGA XBT lines in the Indian Ocean* CSIRO Marine Laboratories Report xxx (in preparation).

6. Semtner, A.J. and R.M. Chervin (1988) *J. Geophys. Res.*, **93**, 15502-15522; Inoue, M. and S.E. Welsh (1993) *J. Phys. Oceanogr.* (in press); Clarke, A.J. and X. Liu (1993) *J. Phys. Oceanogr.* (in press); Masumoto and Yamagata (1993) (submitted).

7. Wyrtki, K. (1987), *J. Geophys. Res.*, **92**, 12941-12946.

8. Qu, T., G. Meyers, J.S. Godfrey and D. Hu (1993) (submitted).

9. Wyrtki, K. (1973) *Science* **181**, 262-264.

10. Murray, S.P. and D. Arief (1988) *Nature* **333**, 444-447. Their annual phase did not indicate a maximum southward flow in May. The discrepancy my be due to the relatively short duration (1 year) of the current meter mooring.

11. Perigaud, C. and P. Delecluse (1993) *J. Geophys. Res.*, **97**, 20169-20178.

ACKNOWLEDGMENTS:
Volunteer observers on merchant ships have generously collected the XBT data. Substantial external resources were provided by Royal Australian Navy, Department of the Environment (Australia), Bureau of Meteorology (Australia), NOAA (USA), Ministry of Education (Japan) and Japan Meteorological Agency. An XBT network to monitor throughflow was first suggested by Dr J.S. Godfrey, and his comments have been helpful throughout the study. Discussions with Drs G. Cresswell, J. R. Donguy and F Schott were helpful.

Captions

Figure 1. Tracklines (Sections A, B and C) in the Indonesian region monitored by expendable bathythermograph.

Figure 2. Mean temperature sections. Section A top, Section B middle, Section C bottom.

Figure 3. Geostrophic volume transports relative to 400 m in 10^6 m^3/s.

Figure 4. TOP. Variation of South Equatorial Current (SEC, westward), South Java Current (SJC, eastward), eastern gyral current (EGC, eastward) and Leeuwin Current (LC, southward), in 10^6 m^3/s, on Section A. MIDDLE. Net relative transport (0/400 m) from continental shelf to shelf on sections A and C. BOTTOM. Depth of the 20°C isotherm averaged on sections A and B between NW Australia and Java/Timor.

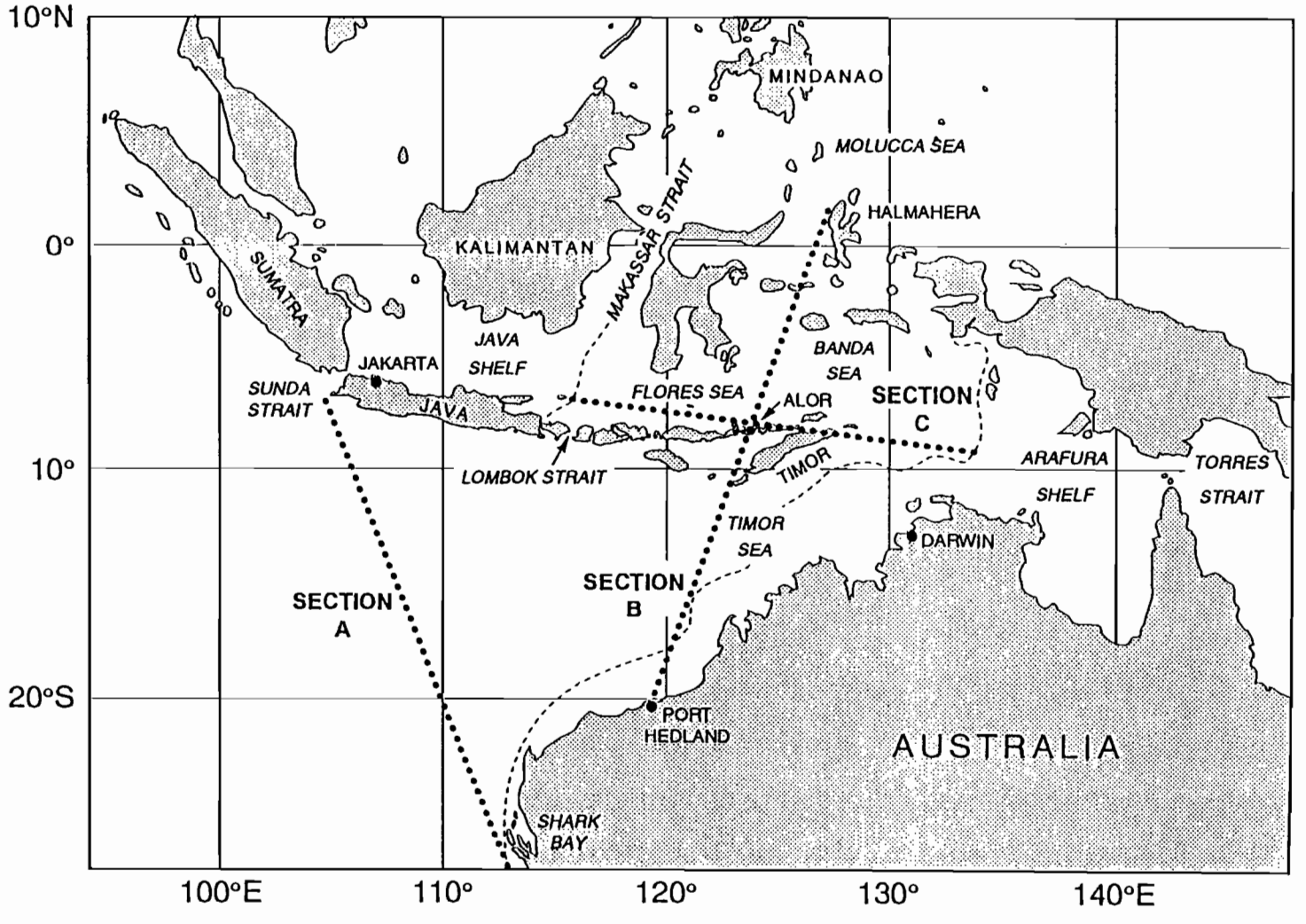

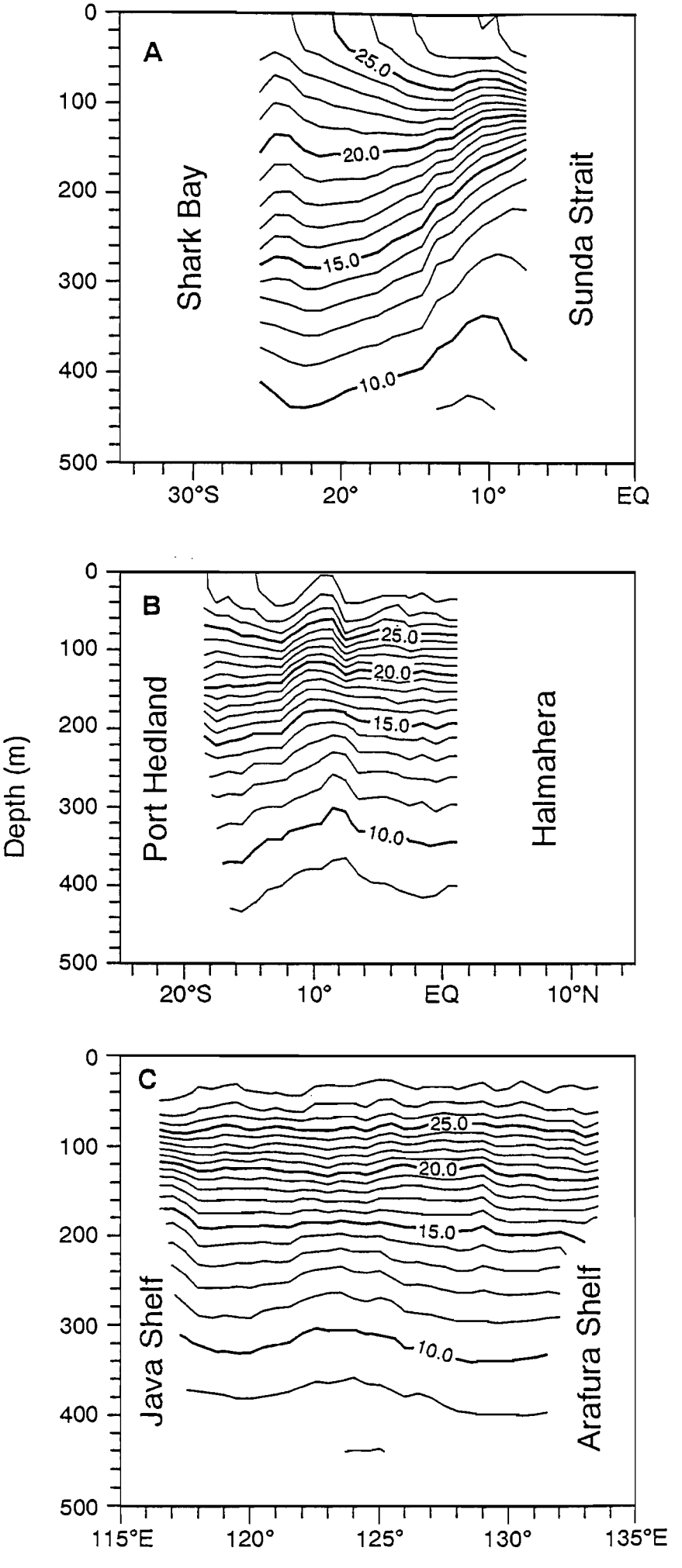

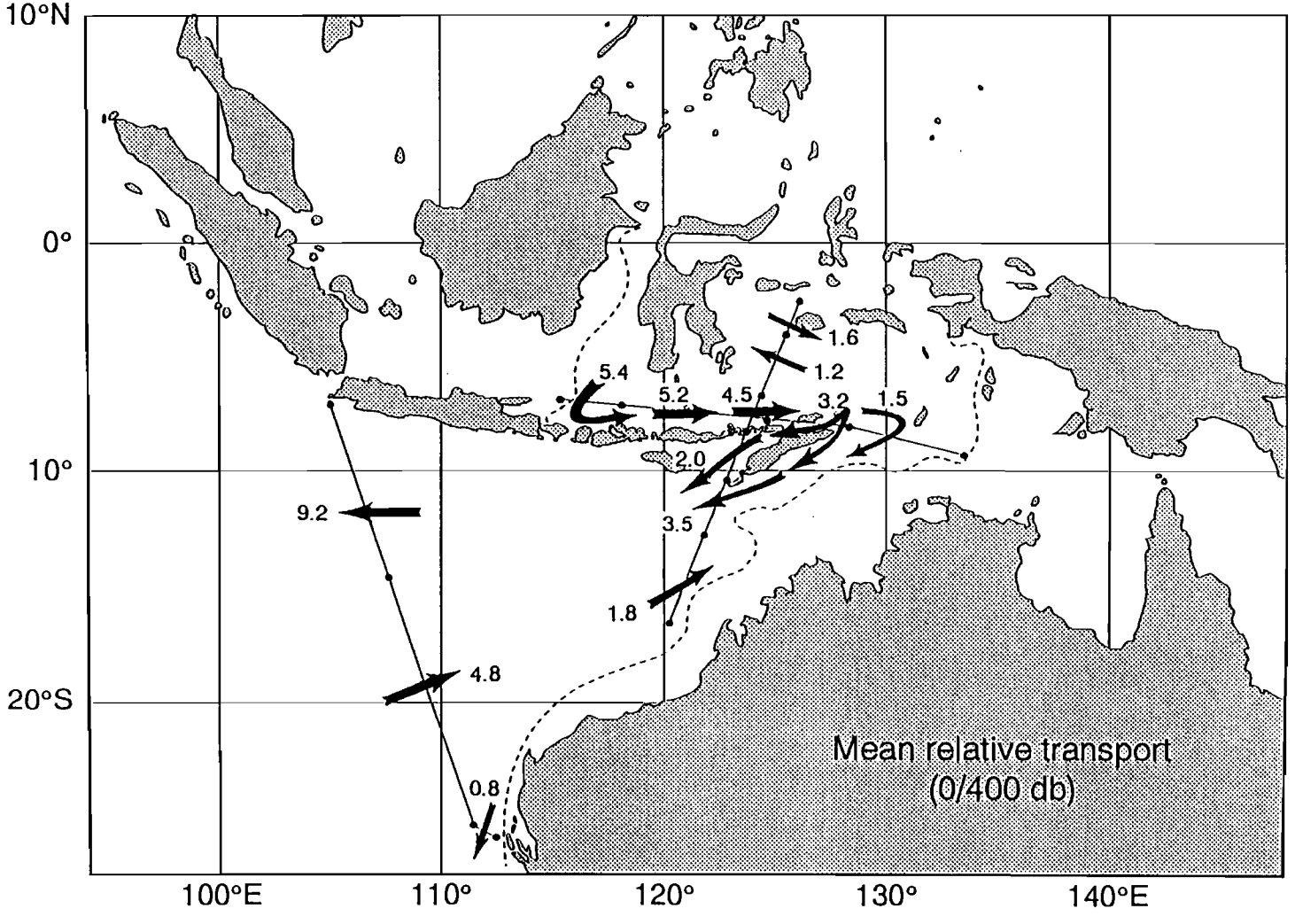

(4)

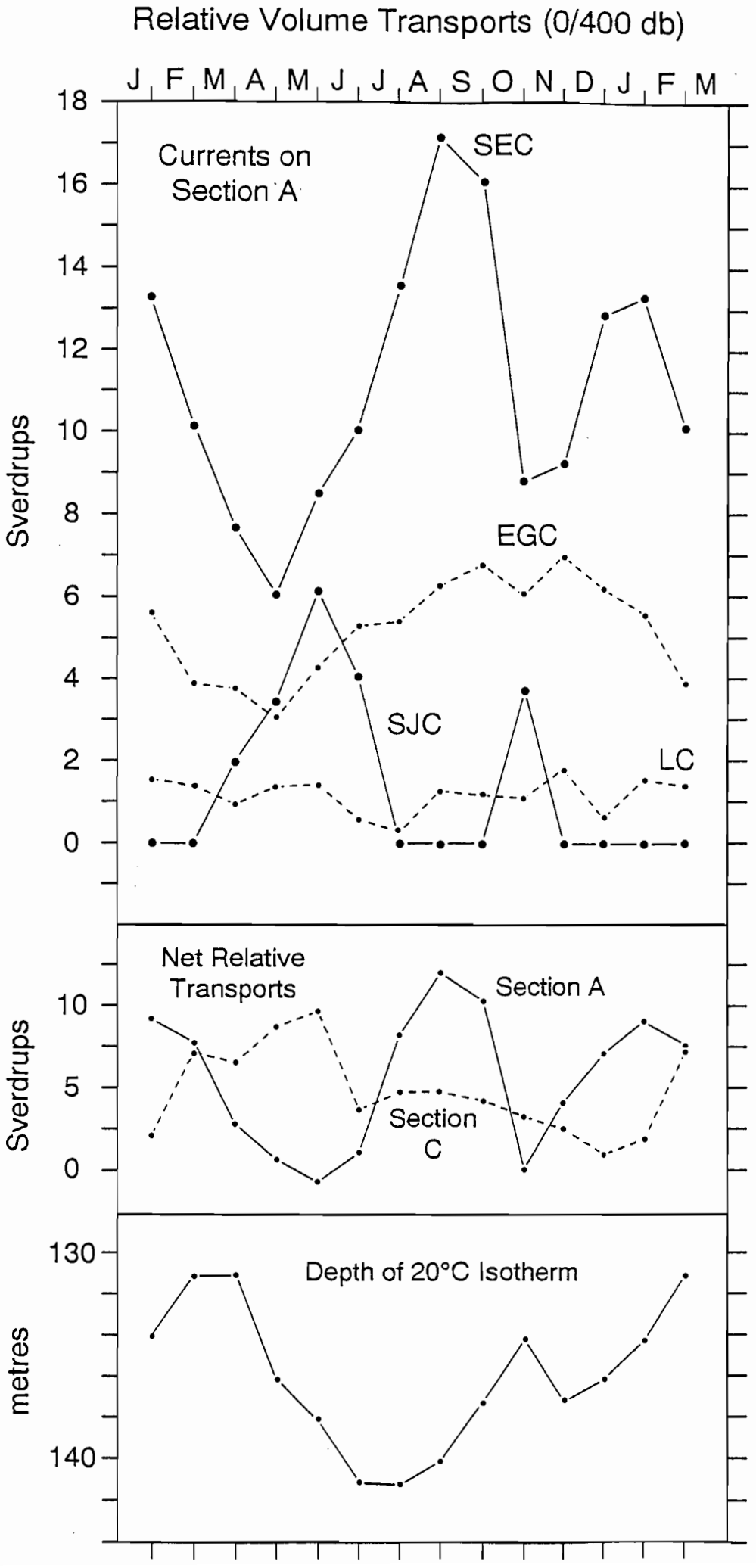

Donguy Jean-René, Meyers G. (1993).

Transport-regime in the western tropical Indian Ocean.

In : Meyers G., Bailey R.J., Worby A.P. Volume transport of Indonesian throughflow.

s.l. : s.n., 17 p. multigr.